Pharmaceutica Analytica Acta
ISSN: 2153-2435

Yadav et al., Pharm Anal Acta 2015, 6:9
DOI: 10.4172/2153-2435.1000419

Research Article Open Access

Vibrational Studies and DFT Calculations of Cytosine, Thiocytosine and Their Cations and Anions

Yadav RA*, Rashmi Singh and Mayuri Srivastava

Department of Physics, Banaras Hindu University, Varanasi-221005, India

Abstract

DFT calculations were carried out to compute the optimized molecular geometries, APT charges and fundamental vibrational frequencies along with their corresponding IR intensities, Raman activities and depolarization ratios of the Raman bands for the neutral Cyt and TCyt molecules and their cations and anions using the DFT/B3LYP method with the 6-311++G** basis set using the Gaussian-03 software. TCyt, Cyt^+ and $TCyt^+$ show planar structures and belong to C_s point group symmetry while Cyt, Cyt^- and $TCyt^-$ possess non-planar structures with C_1 point group symmetry. Conformational analysis was carried out to obtain the most stable configurations of these molecules. The normal modes of vibration for all the species have been assigned on the basis of PEDs obtained from normal coordinate analysis using the GAR2PED software. Information about the size, shape, charge density distribution and site of chemical reactivity of the molecule has been obtained by mapping the electron density isosurface with molecular electrostatic potential (MEP) surfaces. The energy gap from HOMO to LUMO of the Cyt is 5.2963 eV and that of TCyt is 5.0062 eV.

Keywords: Cytosine; Thiocytosine; Vibrational characteristics; PEDs; HOMO-LUMO; MEP

Abbreviations

APT: Atomic Polar Tensor; B3LYP: Becke3-Parameter (Exchange), Lee, Yang, Parr (Correlation); DFT: Density Functional Theory; ED: Electron Density; FTIR: Fourier Transform Infrared Spectroscopy; HOMO: Highest Occupied Molecular Orbital; LUMO: Lowest Unoccupied Molecular Orbital; MEP: Molecular Electrostatic Potential; MOs: Molecular Orbitals; PED: Potential Energy Distribution; DNA: Deoxyribose Nucliec Acid; RNA: Ribose Nucliec Acid; Cyt: Cytosine; Cyt^+: Cytosine Cation; Cyt^-: Cytosine Anion; TCyt: Thiocytosine; $TCyt^+$: Thiocytosine Cation; $TCyt^-$: Thiocytosine Anion

Introduction

Cytosine (Cyt) is the smallest molecule which is common in both the RNA and DNA polymers. Cytosine and its derivatives are the compounds of great biological importance as these are constituents of nucleic acids. Cytosine molecule is the most alkaline in aqueous solution and this particular feature plays an important role in many biochemical processes. Sulfur is a very reactive element and it is used as chemical warfare agent. As a result, it strongly interacts with RNA and DNA chain molecules. Most of the investigations on sulfur containing compounds of Cyt have focused on the study of thiocytosine (TCyt).

The properties of the cations that are generated from the neutral nucleobases molecules during certain processes help in understanding the nucleic acids in different environments and conditions. The location of the initial charges in DNA and RNA largely affects and governs the creation of neutral nucleotide radicals. These radicals are formed by protonation of the radical anions and deprotonation of the radical cations [1-3]. Cyt molecule has been studied by Barker and Marsh [4] to determine its crystal structure. Furberg and Jensen [5] studied the X-ray diffraction of the TCyt molecule to establish its crystal structure. Estrin et al. [6] have determined all the possible tautomeric forms of the uracil and Cyt molecules using DFT method. The IR and Raman spectra of the Cyt molecule have been studied and analyzed by Susi et al. [7]. They have also studied the Raman spectrum of polycrystalline Cyt in the range 300-3300 cm^{-1}. Nowak et al. [8] have analyzed the IR frequencies observed in the Ne and Ar matrices and proposed vibrational assignments for the isolated Cyt molecule. The IR spectrum of TCyt has been recorded and analysed in powder form in the range of 400-4000 cm^{-1} and the Raman spectrum in the range 40-4000 cm^{-1} in our laboratory in the past [9]. Kwiatkowski and Leszczynski have investigated the vibrational spectra of Cyt and its thio and seleno analogues [10]. Subramanian et al. [11] have performed semi-empirical quantum mechanical calculations of vibrational IR spectra of Cyt and TCyt. The quantum mechanical calculation of Cyt was done by Florian et al. [12] to interpret experimental IR and Raman spectra. Szczesniak et al. [13] have carried out the matrix isolation and ab initio studies of the infrared spectra of Cyt monomers. Czerminski et al. [14] have carried out the quantum- mechanical studies of the structures of Cyt dimers and Gua-Cyt pairs. The matrix isolation and theoretical studies of the IR spectra and tautomerism of 5- halo Cyt have been made by Jaworski et al. [15]. Radchenko et al. [16] have interpreted the experimental and theoretical studies of molecular structure features of cytosine. Stepanian et al. [17] have studied and compared the theoretical and experimental studies of adenine, purine and pyrimidine isolated molecular structures. Gould et al. [18] have predicted the IR spectra of Cyt tautomers theoretically. A theoretical investigation of tautomeric equilibrium and proton transfer in isolated and hydrated TCyt have been done by Podolyan et al. [19]. Krishnkumar and Balachandran [20] have analyzed the vibrational spectra of 5-haloCyt with the help of DFT method. Rostkowska et al. [21,22] interpreted the matrix isolation experimental and theoretical studies on TCyt and 5-fluro TCyt.

***Corresponding author:** Yadav RA, Department of Physics, Banaras Hindu University, Varanasi-221005, India, Tel: +91-542-2368593; Fax: +91-542-2368390; E-mail: ray1357@gmail.com, rayadav@bhu.ac.in

Received July 09, 2015; **Accepted** August 18, 2015; **Published** August 21, 2015

Citation: Yadav RA, Singh R, Srivastava M, Gondwal M (2015) Vibrational Studies and DFT Calculations of Cytosine, Thiocytosine and Their Cations and Anions. Pharm Anal Acta 6: 419. doi:10.4172/21532435.1000419

In spite of several studies on the vibrational spectra there are several inconsistencies in the assignment of fundamental frequencies of the cytosine and thiocytosine molecules. In order to make consistent vibrational assignments for the fundamental modes of these two molecules, we have carried out DFT calculations at the B3LYP/6-311++G** level. We have also included singly charged cations and anions of the Cyt and TCyt molecules for the present study. The aim of the present work is 2-fold. Firstly we have reanalyzed the earlier reported IR and Raman spectra of the Cyt and TCyt molecules and correlated the observed IR and Raman frequencies to the calculated fundamental frequencies. Secondly the structural and vibrational features for the radicals of these two molecules are compared with those of the neutral molecules. Similar works for the uracil, some organic superconductor and vitamins have also been done by our group recently [23-30].

Computational Details

The DFT calculations were carried out to compute the optimized molecular geometries, APT charges and fundamental vibrational frequencies along with their corresponding IR intensities, Raman activities and depolarization ratios of the Raman bands for the neutral Cyt and TCyt as well as their radical ions (Cyt, Cyt^+, Cyt^-, TCyt and $TCyt^+$) using Gaussian-03 software [31]. For the Cyt molecule, the initial parameters were taken from the work of Barker et al. [4] and calculations were performed at the B3LYP/6-31+G* level [32,33]. In the optimized geometry at the B3LYP/6-311++G** level for the Cyt molecule, the O atom was replaced by an S atom at the carbon site C_2 with the C=S bond length 1.664Å [23] and with this modification the optimized geometry at the B3LYP/6-311++G** level for the Cyt molecule is taken as the input structure for the neutral TCyt molecule for the DFT calculation at the B3LYP/6-311++G** level by taking charge 0 and multiplicity 1. For the radical cations of both the molecules, the input structures were taken from the geometries of their corresponding neutral molecules optimized at the B3LYP/6-311++G** level and the DFT calculations were performed at the B3LYP/6-311++G** level by taking the charge as +1 and multiplicity as 2. For the computations of different parameters of our interest for the anions of these molecules computations are performed at the B3LYP/6-311++G** level by taking the input structures from the geometries of their corresponding neutral molecules, as for the anion, and the charge as -1 and multiplicity as 2. The assignments of the normal modes of vibration for all the three molecules have been made by visual inspection of the individual mode using the Gauss View software [34]. The numbering scheme for the Cyt and TCyt molecules are shown in Figure 1. The assignments of all the normal modes of vibration have been made on the basis of the calculated potential energy distributions (PEDs). For the calculation of the PEDs the vibrational problem was set up in terms of internal coordinates using the GAR2PED software. The observed IR and Raman frequencies corresponding to the fundamental modes have been correlated to the calculated fundamental frequencies in light of the PEDs. Charge transfer occurring in the molecule has been shown by calculating the energy difference between the highest occupied molecular orbital (HOMO) and the lowest unoccupied molecular orbital (LUMO).

Results and Discussion

Molecular geometries and APT charges

The optimized geometrical parameters for the Cyt, TCyt and their corresponding radicals calculated at the B3LYP/6-311++G** level along with the experimental parameters for the Cyt and TCyt molecules are collected in Table 1.

Neutral TCyt and cations of Cyt and TCyt show planar structures and belong to C_s point group symmetry while the neutral Cyt and anions of Cyt and TCyt possess non-planar structure with C_1 point group symmetry.

One can see from the Table 1, a small difference in geometries of the anionic and cationic species from the neutral species. The major changes of the bond lengths for all the species are clearly shown in Figure 2.

Atomic polarizability tensor (APT) is interpreted as sum of the charge tensor and charge flux tensor, leading to a charge-charge flux model. The magnitude of the APT charges of neutral, cationic and anionic species are collected in Table 2 and these APT charges are pictorially shown in Figure 3.

Neutral molecules: A perusal of the Table 1 shows that there is no change in bond lengths C-H and N-H in going from Cyt to TCyt. The bond lengths N_1-C_6, N_1-C_2 and N_3-C_2 decrease by 0.001 Å, 0.21 Å and 0.015 Å for TCyt as compared to Cyt while the bond lengths N_3=C_4 increases slightly (by 0.006 Å). Because of less electronegativity of S atom (-0.682) as compared to the O atom (-0.923), the atomic charges decrease by 0.008, 0.211, 0.098, 0.014, 0.002, 0.004and 0.061 atomic unit on the sites N_1, C_2, N_3, C_5, C_6, H_7 and N_9 respectively while the atomic charges increase by 0.122, 0.241, 0.004, 0.004, 0.005 and 0.011 atomic unit on the sites C_4, S_8, N_9 and $H_{10/11/12/13}$. Due to increased atomic charges bond lengths are decreased. The bond length C_4-C_5 is shortened slightly (by 0.003 Å) because of the opposite character of charges on the site C_4 and C_5. The atomic charges increase on the C_4 site which attracts electronic charges from the C_5 site towards itself. The bond length C_5=C_6 increases by 0.002 Å due to decreased atomic charge on the site C_6. Similarly, there is decrease in the C_4-N_9 bond length. The bond length of C_2-S_8 in TCyt increases by 0.456 Å due to less electronegativity of S atom. The C_2 site pulls the electronic charge from the S atom towards itself. In going from Cyt to TCyt the bond angles vary very slightly. The magnitudes of bond angles of the pyrimidine ring N_1-C_2-N_3, C_5-C_4-N_3 and C_4-C_5-C_6 increase by 0.70 Å, 0.55 Å and 0.29 Å respectively in going from the Cyt to the TCyt molecules. For the neutral Cyt and TCyt, the dihedral angles are indicates the minor

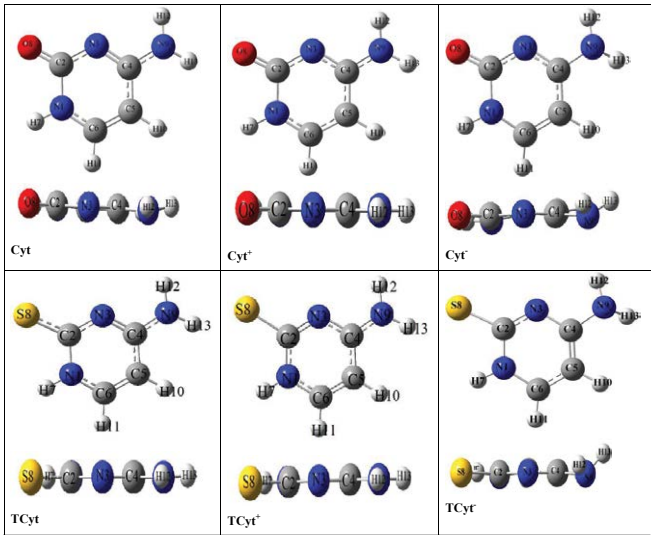

Figure 1: Atomic numbering scheme and front and lateral view of the studied molecules.

Definitions	Cytosine				Thiocytosine			
	Cyt		Cyt^+	Cyt^-	TCyt		$TCyt^+$	$TCyt^-$
	Cal	Exp[6]	Cal		Cal	Exp[7]	Cal	
r (N_1-C_2)	1.428	1.356	1.425	1.423	1.407	1.367	1.366	1.394
r (C_2-N_3)	1.369	1.372	1.345	1.354	1.354	1.343	1.306	1.325
r (N_3-C_4)	1.317	1.354	1.345	1.352	1.323	1.345	1.351	1.383
r (C_4-C_5)	1.440	1.413	1.435	1.407	1.437	1.426	1.432	1.380
r (C_5-C_6)	1.356	1.345	1.387	1.377	1.358	1.354	1.356	1.405
r (C_5-H_{10})	1.080	0.950	1.082	1.085	1.081	0.940	1.081	1.085
r (N_1-C_6)	1.354	1.361	1.330	1.384	1.353	1.355	1.370	1.411
r (C_6-H_{11})	1.083	1.020	1.084	1.082	1.083	0.960	1.082	1.081
r (N_1-H_7)	1.010	0.850	1.018	1.008	1.011	0.860	1.013	1.010
r (C_2-O_8/S_8)	1.216	1.226	1.233	1.236	1.672	1.702	1.743	1.727
r (C_4-N_9)	1.360	1.312	1.331	1.397	1.355	1.332	1.329	1.421
r (N_9-H_{12})	1.008	0.900	1.012	1.015	1.008	0.960	1.011	1.014
r (N_9-H_{13})	1.005	0.800	1.009	1.018	1.005	0.900	1.009	1.014
α (C_6-N_1-C_2)	123.3	122.6	121.5	122.9	123.2	122.0	119.8	123.0
α (C_6-N_1-H_7)	121.4		122.2	120.8	121.4		119.7	120.9
α (N_1-C_6-H_{11})	116.9		118.1	117.8	116.7		116.3	117.1
α (N_1-C_6-C_5)	120.0	121.4	119.5	117.6	120.1	120.1	120.1	115.5
α (C_6-C_5-H_{10})	121.5		119.7	120.9	121.5		120.7	120.2
α (C_6-C_5-C_4)	116.1	118.1	118.4	117.3	115.8	116.7	117.4	118.5
α (C_5-C_4-N_9)	119.0	123.5	121.9	120.5	119.8	119.2	122.2	122.5
α (C_5-C_4-N_3)	124.0	118.0	120.8	124.3	123.4	122.3	120.7	124.1
α (C_4-N_9-H_{12})	117.6	116.0	118.9	111.5	118.1		119.3	108.5
α (C_4-N_9-H_{13})	121.4	124.0	122.7	115.2	122.2		122.1	113.0
α (C_4-N_3-C_2)	120.5	124.3	120.2	119.2	120.7	119.3	119.6	118.4
α (N_1-C_2-N_3)	116.1	115.5	119.6	117.3	116.8	119.6	122.4	119.9
α (N_1-C_2-O_8/S_8)	118.3	123.4	116.4	117.2	118.3	117.6	120.8	116.0
δ(C_2-N_1-C_6-H_{11})	180.0		180.0	-168.6	180.0		180.0	172.0
δ(C_2-N_1-C_6-C_5)	0.0		0.0	13.2	0.0		0.0	10.0
δ(H_7-N_1-C_6-H_{11})	0.0		0.0	-4.1	0.0		0.0	-23.3
δ(H_7-N_1-C_6-C_5)	-180.0		180.0	177.7	180.0		180.0	174.7
δ(C_6-N_1-C_2-N_3)	0.2		0.0	-11.8	0.0		0	-7.6
δ(C_6-N_1-C_2-O_8/S_8)	180.0		180.0	169.1	180.0		180.0	172.7
δ(H_7-N_1-C_2-N_3)	-179.8		180.0	-177.1	-180.0		180.0	-173.3
δ(H_7-N_1-C_2- O_8/S_8)	0.0		0.0	3.8	0.0		-0.1	7.0
δ(N_1-C_6-C_5-H_{10})	179.6		180.0	179.1	180.0		180.0	174.3
δ(N_1-C_6-C_5-C_4)	0.0		0.0	-4.5	0.0		0.0	-6.4
δ(H_{11}-C_6-C_5-H_{10})	-0.4		0.0	1.0	-0.1		0.0	13.8
δ(H_{11}-C_6-C_5-C_4)	-180.0		180.0	177.4	-180.0		180.0	-167.0
δ(C_6-C_5-C_4-N_9)	179.0		180.0	176.4	-180.0		180.0	-179.4
δ(C_6-C_5-C_4-N_3)	-0.2		0.0	-5.5	-0.1		-0.1	1.0
δ(H_{10}-C_5-C_4-N_9)	-0.7		0.0	-7.2	-0.2		-0.1	-0.1
δ(H_{10}-C_5-C_4-N_3)	-179.8		180.0	171.0	-180.0		180.0	-179.8
δ(C_5-C_4-N_9-H_{12})	174.3		180.0	156.4	178.5		180.0	164.0
δ(C_5-C_4-N_9-H_{13})	10.6		0.0	26.7	3.0		0.1	41.4
δ(N_3-C_4-N_9-H_{12})	-6.6		0.0	-21.8	-1.8		-0.1	-16.4
δ(N_3-C_4-N_9-H_{13})	-170.3		180.0	-151.5	-177.4		180.0	-139.0
δ(C_5-C_4-N_3-C_2)	0.4		0.0	7.0	0.1		0.1	1.8
δ(N_9-C_4-N_3-C_2)	-178.8		180.0	-175.0	-180.0		180.0	-178.0
δ(C_4-N_3-C_2-N_1)	-0.3		0.0	1.6	-0.1		0.0	-178.8
δ(C_4-N_3-C_2- O_8/S_8)	180.0		180.0	-179.5	180.0		180.0	1.5

Table 1: Experimental and Calculated Structural Parameters* of Cyt, TCyt and their cations and anions.

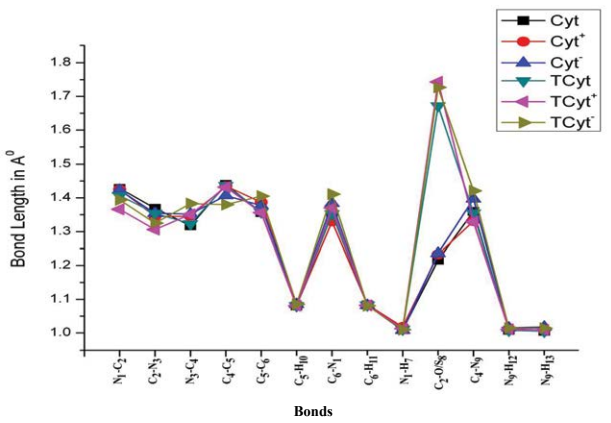

Figure 2: Variations of bond lengths in different molecules.

S No.	Atom	Cyt	Cyt$^+$	Cyt$^-$	TCyt	TCyt$^+$	TCyt$^-$
1	N_1	-0.651	-0.094	-1.005	-0.659	-0.602	-0.512
2	C_2	1.337	0.064	0.713	1.126	1.046	0.935
3	N_3	-0.903	-0.156	-1.248	-1.001	-0.913	-1.003
4	C_4	1.129	0.357	1.277	1.251	1.181	0.800
5	C_5	-0.463	-0.082	-0.700	-0.477	-0.389	-0.082
6	C_6	0.457	0.278	1.911	0.455	0.428	-0.067
7	H_7	0.228	0.327	-0.306	0.224	0.265	0.189
8	O_8/S_8	-0.923	0.055	-1.092	-0.682	-0.041	-0.881
9	N_9	-0.787	-0.599	1.261	-0.838	-0.783	-0.583
10	H_{10}	0.057	0.130	-0.372	0.061	0.105	-0.003
11	H_{11}	0.057	0.144	-0.430	0.061	0.121	-0.019
12	H_{12}	0.233	0.296	-0.282	0.238	0.289	0.159
13	H_{13}	0.230	0.281	-0.727	0.241	0.293	0.068

*in electron unit

Table 2: APT Charges* at various atomic sites of Cyt, TCyt and their cations and anions.

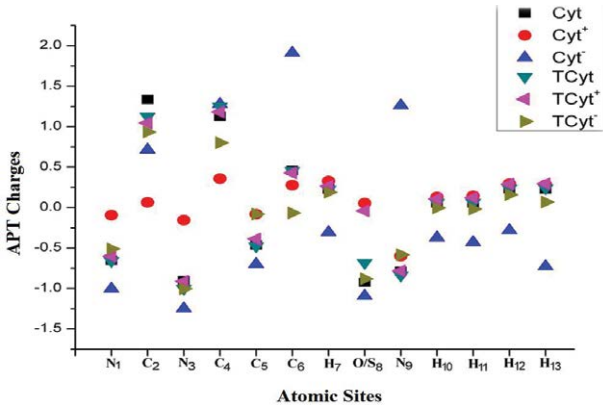

Figure 3: Variations in APT charges at various atomic sites.

change in the molecular structure. The angles C_5-C_4-N_9-H_{12} (174.3°) and N_3-C_4-N_9-H_{13} (-170.3°) show that the two H-atoms of the NH_2 group are not lying in the same plane (containing (N_9, C_4, C_5, C_6, N_1, C_2, N_3, O_8/S_8, H_7, H_{10} and H_{11} atoms).

Cationic species: Conversion of the neutral molecules into their radical cations leads to significant changes in bond lengths and bond angles. Detachment of an electron from the Cyt and TCyt molecules leads to redistribution of the atomic charges in Cyt$^+$ and TCyt$^+$ which results in increase in magnitudes of atomic charges on most of the atomic sites. However, the atomic charges in both species decrease by 1.273, 0.772 and 0.179 atomic units on the C_2, C_4 and C_6 sites. The O/S atom lose more electronic charge and gain positive charge (0.978/0.641) in the process of cationic radicalization. Higher electronegativity of the O / S atom causes increase in the C_2=O/S bond length by 0.017/0.071 Å in Cyt$^+$/TCyt$^+$ radicals. The N atom has more electronegative characters than the C atom which results in the electron pull by N atoms towards themselves from the C atoms. It is noticed that in the case of Cyt$^+$, the N_1-C_2, N_1-C_6, N_3-C_2, C_5-C_4 and C_4-N_9 bond lengths are decreased by 0.003, 0.024, 0.024, 0.005 and 0.029 Å respectively but the N_3-C_4 / C_5-C_6 bond lengths increase by 0.028/0.031 Å respectively. On the other hand in case of TCyt$^+$, the N_1-C_6 / N_3-C_4 bond lengths increase by 0.017/0.028 Å respectively while the N_1-C_2, N_3-C_2, C_4-N_9, C_5-C_4 and C_5-C_6 bond lengths are decreased by 0.041, 0.048, 0.026, 0.005 and 0.002 Å respectively. This is because of the electronic charges which are pulled by the N atom of the amino group towards itself from the C_4 site. It can be seen from the Table 1 that the C_4-C_5 bond length is slightly decreased and the C_5-C_6 bond length increased due to loss of its double bond character in the Cyt$^+$ radical. Due to increase in the atomic charges on the sites N_1, N_3, C_5 and N_9 (0.557, 0.747, 0.381 and 0.188 atomic unit respectively) the N-H/C-H bond lengths are increased by 0.004/0.008Å in the Cyt$^+$ as compared to the neutral molecule. However, the N-H bondlengths of the amino group are increased by 0.003- 0.004 Å in the TCyt$^+$ than that of neutral molecule.

Due to decrease in the N-C bond length, the angle C_6-N_1-C_2 also decreases in the Cyt$^+$ and TCyt$^+$ radicals. In the radicalization process the electronic charge from the C_4 site is dragged by N_9 atom thereby results in shortening of the N_3-C_4-C_5 bond angle in the Cyt$^+$ and TCyt$^+$ as compared to their neutral molecule. The increment in the bond angle N_1-C_2-N_3 results owing to the lengthening of the C_2=O/S bond. Similar result is also observed in the case of C_4-C_5-C_6 bond angle for both the cationic radicals Cyt$^+$ and TCyt$^+$. It can be seen from the Table 1 that the bond angle N_1-C_2-O_8 which decreases by 1.9^0 for the Cyt$^+$ radical while the bond angle N_1-C_2-S_8 is increases by 2.5^0 in TCyt$^+$. For the Cyt$^+$ radical, the change in bond angle N_1-C_2-O_8 is larger than that of Cyt molecule owing to increases in polarity of N_1 and O_8 and attracts each other. The increment of 1.3^0 in the C_4-N_9-H_{12} and C_4-N_9-H_{13} bond angles because of repulsion between the atoms C_4 and H_{12}/H_{13} in going from the neutral Cyt to Cayionic Cyt. For the TCyt$^+$ C_4-N_9-H_{12} increases by 1.2 and the C_4-N_9-H_{13} bond angle is nearly equal to the neutral TCyt molecule. For the cationic Cyt and TCyt species, the angles C_5-C_4-N_9-H_{12}, C_5-C_4-N_9-H_{13}, N_3-C_4-N_9-H_{12} and N_3-C_4-N_9-H_{13} are either 0° or ± 180° which shows the atoms N_3, C_4, C_5, N_9, H_{12} and H_{13} are in same plane with the molecular plane.

Anionic species: As can be seen from the Table 1 and Table 2, conversion of the neutral Cyt and TCyt molecules in their radicals anion leads to significant changes in their APT charges (Table 2) and the geometrical parameters (Table 1). Due to redistribution of atomic charges of Cyt$^-$ radical, at the sites C_4, C_6 and N_9 positive magnitude of charges increase by 0.148, 1.454 and 2.048 atomic unit respectively while all the other atoms show decrease. The atomic charges on N_1/N_3 increase in the negative magnitudes by 0.354/0.345 atomic unit while the charges on C_2 is decreased by 1.024 atomic unit which results in a significant decrease in the bond lengths of N_1-C_2/C_2-N_3 by 0.005/0.015 Å in Cyt$^-$ and 0.013/0.029 Å in TCyt$^-$. The bond lengths N_3-C_4/N_1-C_6 in

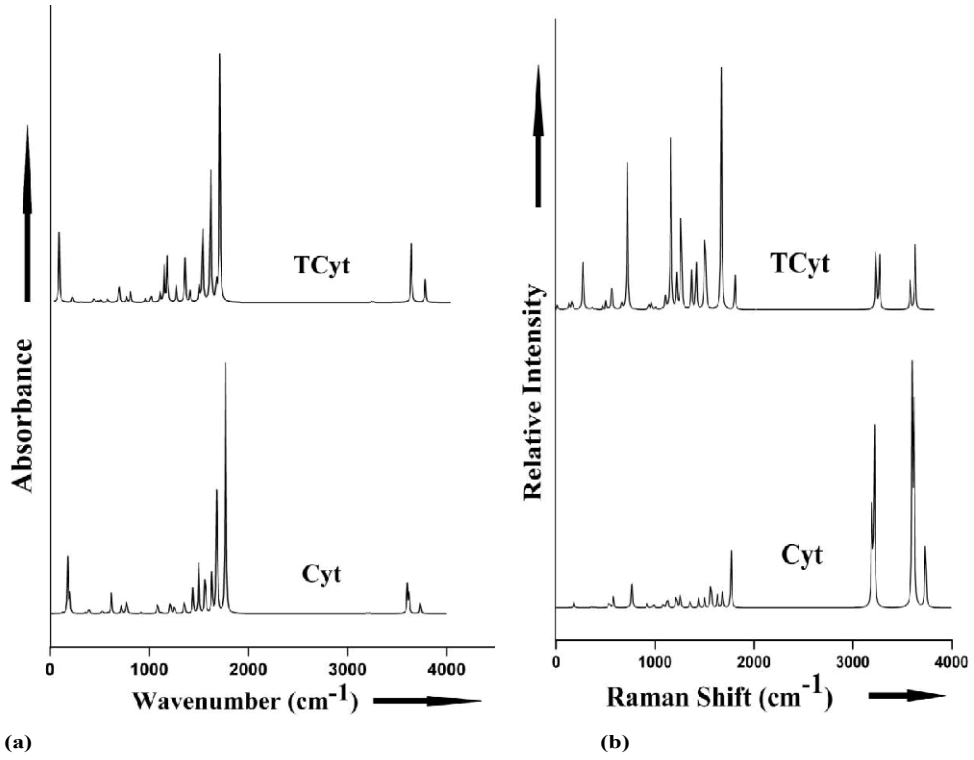

Figure 4: Calculated IR and Raman spectra of Cyt and TCyt.

anionic radical of Cyt are lengthened by 0.035/0.030 Å due to repulsion between N_3 and H_{12} and N_1 and H_{11} atoms. The process of radicalization leads to decrease in C_4-C_5 bond length by 0.033/0.057Å in Cyt / TCyt radical anions as compared to their neutral molecules due to opposite sign of charges on the C_4 (1.277) and C_5 (-0.700) sites. The C_2=O/S_8 bond length is found to increase by 0.020 and 0.025Å for radical anions of Cyt^- and $TCyt^-$ respectively as compared to their neutral molecules. The bond lengths N_9-H_{12}/N_9-H_{13} of the amino group increase by 0.007 Å/0.013 Å in Cyt^- and 0.006/0.009 in $TCyt^-$ respectively than those bond lengths of Cyt and TCyt molecules.

The magnitudes of bond angle C_2-N_1-C_6 increases by 0.4^0 and 0.2^0 due to the lengthening of C_2=O/S_8 bond in both anions. Increment of 1.2^0 is noted for the bond angles N_1-C_2-N_3 and C_4-C_5-C_6 due to the radicalization process which results in the lengthening of bonds C_2=O_8 and C_5-H_{10} in Cyt^- radical. For $TCyt^-$ the two N_1-C_2-N_3 and C_4-C_5-C_6 bond angles increase by magnitudes 3.1^0 and 2.7^0 respectively. Due to the radicalization process the magnitude of bond angle C_5-C_4-N_9 increases in the anionic Cyt. Decrement of 1.1^0 and 1.3^0 in the bond angles N_1-C_2-O_8 and C_4-N_3-C_2 in the anionic Cyt radical. The bond angle C_6-C_5-H_{10} increases by 0.6 in Cyt^- but decreases by 1.3 in $TCyt^-$ than that of neutral molecules. Major changes are calculated in the dihedral angles for the radical anion of Cyt and TCyt molecules. Variations in the dihedral angles show that the two H atoms of NH_2 group and C_4, N_9 of the studied molecules are not in same plane. Thus, it has been found that both H atoms of NH_2 group lies above the molecular plane containing N_9, C_4, C_5, C_6, N_1, C_2, N_3, O_8/S_8, H_7, H_{10} and H_{11} atoms. However, in case of anions of studied molecules, the dihedral angles C_5-C_4-N_9-H_{12} (164.0°) and N_3-C_4-N_9-H_{13} (-139.0°) indicates that the both H atoms are lying only one side of the molecular plane.

Vibrational analysis

Neutral TCyt and cations of Cyt and TCyt show planar structures and belong to C_s point group symmetry and all the 33 normal modes are distributed between the two species as: 23a′+10a″. The neutral Cyt and anions of Cyt and TCyt possess non-planar structure with C_1 point group symmetry and all the 33 normal modes fall under a single species and therefore, the distribution is given by -33a.

All the modes are IR as well as Raman active. The calculated vibrational frequencies, IR intensities, Raman activities and depolarization ratios of the Raman bands for the neutral and radicals species of the Cyt and TCyt molecules computed at the B3LYP/6-311++G** level are given collected in Table 3, which also includes the observed fundamental frequencies for the two neutral molecules reported earlier [9-11]. Table 4 presents the computed PEDs for all the 33 modes of the studied molecules.

As one gets the Raman activities (S_i) from the quantum chemical calculations, the corresponding Raman intensities (I_i) are calculated using the relation [34,35],

$$I_i = \frac{f(\nu_0 - \nu_i)^4 S_i}{\nu_i\left[1-\exp\left(-hc\nu_i / kT\right)\right]} \quad (1)$$

where ν_0 is the excitation frequency (in cm^{-1}), ν_i is the vibrational frequency (in cm^{-1}) of the i^{th} normal mode; h, c and k are the Planck constant, the speed of light and the Boltzmann constant, respectively, T is the absolute temperature and f is some suitably chosen scaling factor common for all the peak intensities. The computed IR and Raman spectra for the Cyt and TCyt molecules and their corresponding radicals are shown in Figure 4 and Figure 5.

Neutral molecule: In the following the vibrational assignments in light of the presently calculated frequencies and earlier experimental IR and Raman spectra [9,11] for the neutral Cyt and TCyt molecules have been discussed in detail. All these data are presented in the Table 3.

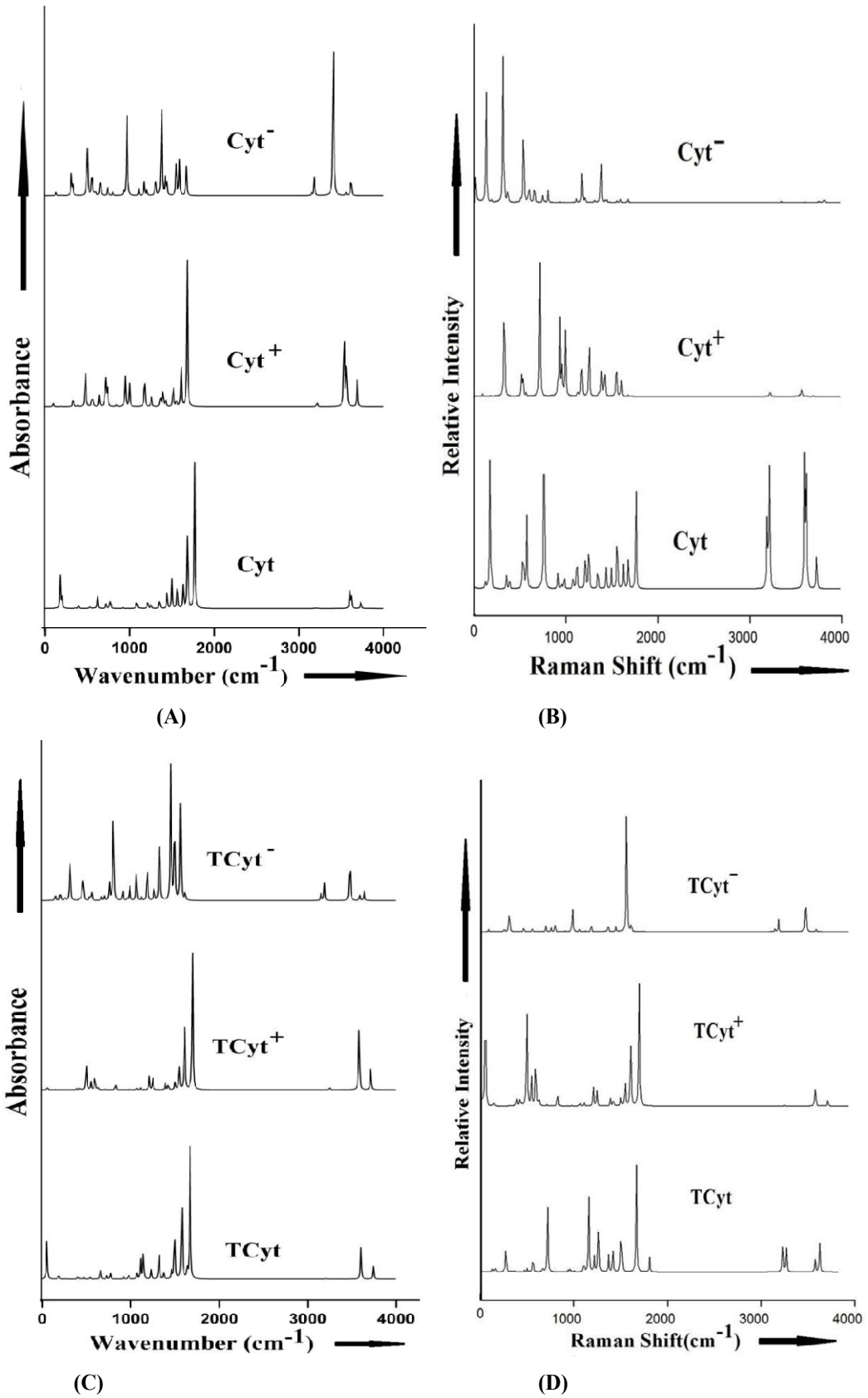

Figure 5: Calculated IR and Raman Spectra of Cyt, TCyt and their cations and anions.

Modes	Cytosine				Thiocytosine				Assignments
	Cyt		Cyt^+	Cyt^-	TCyt		$TCyt^+$	$TCyt^-$	
	Cal	Exp[9]	Cal		Cal	Exp[11]	Cal		
ν_1	128 (2,0) 0.75	123(R,vvw)	98 (11,1) 0.75	130 (152,68005) 0.23	111 (0, 0) 0.75	98(R,vw)	147 (4,1) 0.64	89 (1,950) 0.35	φ(ring) a″
ν_2	180 (171,3) 0.20	162 (R,vw)	477 (154, 0) 0.75	555 (1629,512264) 0.25	50 (188, 1) 0.27	50(R,w)	500 (159,1) 0.71	803 (285,3206) 0.27	ω(NH_2) a′
ν_3	200 (55, 0) 0.35		187 (1,0) 0.75	190 (21, 2638) 0.747	185 (23, 0) 0.75		105 (14, 6) 0.68	146 (17, 125) 0.46	φ(ring) a″
ν_4	358 (3,0) 0.65	356 (R,vw)	334 (35,156) 0.749	364 (14,12046) 0.40	438 (3, 3) 0.62	434(IR,ms) 432 (R,w)	421 (7,8) 0.37	424 (7,8) 0.62	β(C-NH_2)
ν_5	395 (21,1) 0.74	421(IR,w) 400(R,w)	386 (5,1) 0.75	312 (1154,404838) 0.23	404 (14, 1) 0.75	422(IR,s) 423(R,w)	398 (8,4) 0.65	305 (27,3537) 0.31	φ(ring) a″
ν_6	525 (11,0) 0.73	520 (IR,sh) 517(R,w)	641 (36, 0) 0.75	329 (496,190998) 0.34	538 (9, 0) 0.63	527 (IR,vs)	594 (87,0) 0.43	205 (27,148) 0.67	τ(NH_2) a′
ν_7	533 (3,2) 0.55	533(IR,m) 533 (R,m)	520 (1 ,46) 0.75	500 (2118,525975) 0.22	269 (1, 3) 0.75		213 (0,3) 0.50	255 (10,1153) 0.31	β(CO/S) a′
ν_8	545 (3,3) 0.44	549(IR,mw) 546(R,mw)	537 (0, 59) 0.54	534 (15,10053) 0.39	555 (1, 7) 0.17	551(IR,s) 550(R,mw)	557 (1,14) 0.20	534 (14,45) 0.50	α (ring) a′
ν_9	579 (3,7) 0.38	566 (IR ,w) 568(R,mw)	571 (18,10) 0.58	578 (70,14401) 0.57	470 (6,17) 0.21	456(IR,vs) 452(R,s)	436 (1,1) 0.15	452 (27,12) 0.74	α (ring) a′
ν_{10}	619 (66,0) 0.16	600(IR,ms) 597(R,vw)	708 (51,0) 0.75	490 (896,48474) 0.26	658 (43, 1) 0.75	652(IR,ms) 659(R,vw)	555 (47,15) 0.65	464 (64,1783) 0.24	γ (N_1H) a′
ν_{11}	723 (30,0) 0.55	701(IR,sh) 704(R,vw)	845 (9, 1) 0.75	802 (175,126126) 0.43	730 (14,2) 0.75	724(IR,mw) 718(R,vs)	823 (35,0) 0.69	758 (50,1690) 0.29	γ (C_5H) a′
ν_{12}	762 (9,5) 0.06	760(IR,msh) 764(R,w)	555 (38,0) 0.75	655 (1120,15899) 0.33	768 (31, 3) 0.74	752(IR,ms) 755(R,vw)	740 (0,1) 0.68	557 (28,1513) 0.28	γ (C-NH_2) a″
ν_{13}	766 (5,2) 0.06	782(IRmw) 782(R,mw)	721 (83,468) 0.47	742 (440,73423) 0.23	716 (0, 21) 0.06	710(R,ssh)	715 (4,11) 0.14	701 (11,2163) 0.27	ν (ring) a′
ν_{14}	774 (46,1) 0.41	793(IR,ms) 792 (R,s)	737 (75, 1) 0.75	767 (21,6974) 0.55	651 (15, 0) 0.73		625 (2,5) 0.73	669 (9,127) 0.34	γ (CO/S) a″
ν_{15}	919 (5,3) 0.51	894(R,vw)	922 (2,37) 0.71	931 (234,7728) 0.67	920 (11, 3) 0.38	930(IR,ms) 932(R,mw)	929 (1,26) 0.15	908 (26,405) 0.26	ν (ring) a′
ν_{16}	957 (1,1) 0.71	966(IR,w) 971(R,ssh)	991 (0,1) 0.75	595 (234,137124) 0.65	960 (0, 1) 0.75	967(IR,vw) 965(R,mw)	979 (0,0) 0.73	314 (125,6095) 0.28	γ (C_6H) a′
ν_{17}	986 (1,3) 0.25	994(IR,ms) 990(R,ms)	947 (128,166) 0.75	1000 (9, 4882) 0.30	976 (24,7) 0.19	983(IR,mw) 971(R,ms)	985 (2,4) 0.12	958 (5,68) 0.15	α (ring) a′
ν_{18}	1084 (47,3) 0.23		999 (80,356) 0.62	1109 (328,52914) 0.24	1069 (29, 5) 0.10		1065 (11,1) 0.66	1121 (10,327) 0.08	ρ(NH_2) a
ν_{19}	1125 (3,8) 0.30	1100(IR,w) 1108(R,vw)	1135 (0,37) 0.66	1171 (729,461449) 0.32	1109 (100, 4) 0.73	1098(IR,ms) 104(R,ms)	1108 (10,11) 0.25	987 (48,10746) 0.26	β(CH) a′
ν_{20}	1214 (49,10) 0.51	-	1257 (43, 479) 0.74	1438 (724,59563) 0.21	1231 (46, 5) 0.43	1235(IR,s) 1249(R,mw)	1243 (57,5) 0.31	1186 (109,3146) 0.20	β(NH) a′
ν_{21}	1254 (31,3) 0.12	1236(IR,mw) 1247(R,w)	1176 (134,314) 0.73	969 (4096, 0) 0.24	1318 (140, 61) 0.10	1302(IR,vs) 301(R,vs)	1497 (45,7) 0.11	1324 (224,385) 0.67	ν(ring) a′
ν_{22}	1354 (56,6) 0.09	1364(IR,ms) 1361(R,w)	1365 (46,36) 0.61	1420 (812, 33834) 0.21	1371 (33, 4) 0.46	1368(IR,ms) 1370 (R,ms)	1384 (48,5) 0.72	1365 (2, 3289) 0.29	β(CH) a′

ν_{23}	1442 (87,7) 0.19	1465(IR,vs) 1462(R,w)	1393 (64, 282) 0.65	1203 (358, 82892) 0.18	1461 (45,10) 0.42	1460 (IR,s) 463(R,ms)	1416 (37,6) 0.49	1495 (276,136) 0.27	ν(ring) a′
ν_{24}	1499 (155,6) 0.31	1505(IR,s) 1498(R,w)	1516 (91, 8) 0.15	1306 (1109,58525) 0.14	1496 (321,9) 0.14	1505 (IR,sh) 495(R,w)	1541 (170,9) 0.67	1263 (42,146) 0.23	ν(C-NH_2) a
ν_{25}	1564 (169,22) 0.34	1538(IR,ms) 1533(R,ssh)	1555 (29, 420) 0.75	1377 (5367,895702) 0.24	1576 (527, 28) 0.11	1580(IR,vvs) 1582(R,ms)	1601 (461,33) 0.69	1562 (279,47006) 0.23	ν(ring) a′
ν_{26}	1632 (140,9) 0.17	1615(IR,vs) 1612(R,w)	1679 (493, 15) 0.63	1589 (1748, 80132) 0.55	1636 (73, 5) 0.22	1630 (R,w)	1665 (3,12) 0.17	1614 (25,2902) 0.37	σ(NH_2) a
ν_{27}	1683 (508,13) 0.11	1662(IR,vvs) 1653(R,ms)	1609 (133,60) 0.73	1554 (2301, 48957) 0.15	1670 (668, 22) 0.30	1645(IR,vvs) 669(R,ms)	1690 (739,16) 0.18	1452 (377,2197)0.43	ν(ring) a′
ν_{28}	1769 (780,7) 0.29	-	1426 (32,287) 0.68	1668 (1743, 256147) 0.24	1142 (150, 9) 0.21	1163(IR,ssh) 1167(R,sh)	1205 (83,6) 0.30	1063 (85,919) 0.33	ν (CO/S) a′
ν_{29}	3193 (3,81) 0.49	3169(IR,s) 3176(R,ms)	3207 (5, 77) 0.69	3183 (1104, 90876) 0.35	3200 (2, 76) 0.57	3063(IR,ssh) 061(R,vs)	3230 (9,141) 0.17	3189 (46,4664) 0.74	ν(CH) a′
ν_{30}	3218 (2,128) 0.19	3230 (R,vvs)	3217 (12, 124) 0.15	3149 (132, 100464) 0.36	3221 (1, 162) 0.20	3094(IR,vs) 3090(R,vs)	3216 (4,59) 0.61	3152 (22,1241) 0.38	ν(CH) a′
ν_{31}	3601 (93,149) 0.13	3380(IR,vs) 3354(R,vvs)	3564 (192,349) 0.13	3406 (10540,40051)0.12	3605 (47, 253) 0.16	3312(IR,s) 320(R,ms)	3569 (330,83) 0.14	3475 (137,100636)0.28	ν_s(NH_2) a′
ν_{32}	3618 (69,138) 0.22	-	3536 (319,74) 0.40	3615 (1149,331894)0.27	3600 (135,14) 0.35		3578 (54,136) 0.18	3637 (29,1122) 0.24	ν(N_1H) a
ν_{33}	3734 (51,8) 0.70	-	3689 (90,19) 0.48	3556 (206,129271) 0.44	3740 (61, 68) 0.64	3334(IR,vs) 34(R,ssh)	3694 (109,53) 0.68	3588 (16,15900) 0.36	ν_{as}(NH_2) a′

[a] The first and second numbers within each bracket represent IR intensity(IR) and Raman activity (R) while the numbers above and below bracket represent the corresponding calculated frequency and depolarization ratio of the Raman band respectively. .

[b] ν=stretching mode, α=deformation mode, φ=out-of-plane ring deformation mode, β=in-plane bending mode, γ=out-of-plane bending mode, δ=deformation mode, $\rho_{\parallel}$=parallel rocking mode, $\rho_{\perp}$=perpendicular rocking mode, τ=torsion mode

[c] vw: very-weak, w: weak, mw: medium-weak, ms: medium-strong, sh: shoulder, msh: medium-shoulder, ssh: strong shoulder, s: strong, vs: very-strong, vvs: very- very strong.

Table 3: Experimental and Calculated Vibrational frequencies for Cyt, TCyt and their cations and anions.

Help has been taken in the vibrational assignment from the computed PEDs given in the Table 4.

Ring modes: In Cyt and TCyt the pyrimidine consists of 6 ring stretching, 3 in-plane bending and 3 out-of-plane bending modes. The modes $\nu_{27,}$ $\nu_{25,}$ ν_{23} $\nu_{21,}$ ν_{15} and ν_{13} are identified as the ring stretching modes; the modes ν_{17}, $_{9,}$ and ν_8 as the planar ring bending modes and the modes ν_5, $_3$ and ν_1 as the non-planar ring bending modes. The frequency for the mode ν_{27} of the Cyt was observed by Susi et al. [9] in IR and Raman spectra at 1662 and 1653 cm^{-1} respectively, with the present calculated frequency 1683 cm^{-1}. For the TCyt molecule, the frequency for the above mode was observed at 1645 and 1669 cm^{-1} in IR and Raman spectra by Yadav et al. [11] and this mode has been calculated to be 1670 cm^{-1}. For the ring stretching modes ν_{25}, ν_{23} and ν_{15} of Cyt and TCyt, there are small differences in the magnitudes of the calculated vibrational frequencies due to the replacement of the O atom by a S atom. These modes (ν_{25}, ν_{23} and ν_{15}) were calculated to have frequencies 1564, 1442 and 919 cm^{-1} for Cyt and 1576, 1461 and 920 cm^{-1} for the TCyt molecule. The IR intensities increase by factors of ~ 3/~ 2 for ν_{25}/ν_{15}, while for the mode ν_{23} it decreases by a factor of ~ 2 in TCyt than that in the Cyt molecule. The observed IR frequencies for these modes are 1538 cm^{-1} (ν_{25}) and 1465 cm^{-1} (ν_{23}) and the Raman frequencies for the modes (ν_{25}, ν_{23} and ν_{15}) are 1533, 1462 and 894 cm^{-1} [9] for the Cyt molecule while the IR frequencies as 1580, 1460 and 1463 cm^{-1} and the Raman frequencies 1582, 1463 and 932 cm^{-1} [11] corresponds to above modes for the TCyt molecule.

It can be seen from the present calculations, the vibrational frequency for the mode ν_{21} is found to be 1254 cm^{-1} for Cyt but in case of TCyt molecule its value increases by 64 cm^{-1} with increase in the IR intensity and Raman activity by factors of ~ 4 and ~ 20, respectively. We could assign the observed IR/Raman frequencies 1236/1247 cm^{-1} [9] for Cyt and 1302/1301 cm^{-1} [11] for TCyt to the mode ν_{21} respectively. The mode ν_{13} is described as the ring breathing mode and is calculated to be 766 cm^{-1} for Cyt and it decreases by 50 cm^{-1} for the TCyt with increases in the IR intensity. This mode could be correlated to the observed frequency 782 cm^{-1} [9] for the Cyt molecule in IR / Raman spectra and it was observed at 710 cm^{-1} by Yadav et al. [11] for the TCyt molecule in the Raman spectrum only.

The highest planar ring deformation mode (ν_{17}) has been calculated to have frequency 986 cm^{-1} for Cyt and 976 cm^{-1} for the TCyt molecule. For this mode the IR and Raman frequencies were observed at 994 and 990 cm^{-1} [9] for Cyt and 983 and 971 cm^{-1} [11] for the TCyt molecule, respectively. The calculated frequencies 579, 545 and 470, 555 cm^{-1} of Cyt and TCyt correspond to the modes ν_9 and ν_8. These two modes were observed at 566, 549 cm^{-1} in the IR spectrum and 568, 546 cm^{-1} in the Raman spectra for the Cyt molecule [9]. Yadav et al. [11] observed the frequencies 456 and 591 cm^{-1} in the IR spectrum and 452 and 550 cm^{-1} in the Raman spectrum for the TCyt molecule which could be correlated to the modes ν_9 and ν_8.

The non-planar ring deformation modes are identified as the modes

Modes	Cytosine			Thiocytosine		
	Cyt	Cyt^+	Cyt^-		$TCyt^+$	$TCyt^-$
	PED	PED	PED	PED	PED	PED
ν_1	**31φ(ring)+**27φ(ring)+ 22γ(N_1H)+19φ(ring)	**67φ(ring)+**19φ(ring)+ 6γ(C-NH_2)+6γ(N_1H)	**34γ(N_1H)+**32(ring)+ 26φ(ring)	**30φ(ring)+**29φ(ring)+23γ(N_1H)+1 7φ(ring)	**49φ(ring)+**20φ(ring)+ 20γ(C_2S)+9γ(N_1H)	**47φ(ring)+**28γ (N_1H) +11φ(ring) +7φ(ring)
ν_2	**55ω(NH_2)+**20(NH_2)+ 8γ (C-NH_2)	**66ω(NH_2)+**27τ(NH_2)+ 6γ(C-NH_2)	**29ω(NH_2)+**17α(ring)+ 15ν(ring)+6β(CO)+ 6β(C-NH_2)	**49ω(NH_2)+**31τ(NH_2) + 16γ(C-NH_2)	**80ω(NH_2)+** 16τ(NH_2)	**57ω(NH_2)+**14γ(C_5H)+8ν (ring)+8γ (C-NH_2)
ν_3	**45φ(ring)+**20φ(ring)+ 14ω(NH_2)+10φ(ring)	**42φ(ring)+**37φ(ring)+ 13γ(N1H)+5γ(CO)	**41φ(ring)+**23φ(ring)+ 19φ(ring)+6γ(C-NH_2)	**51φ(ring)+**32φ(ring) +7γ(CS)+ 5γ(C_5H)	**67φ(ring)**+18φ(ring)+ 5γ(C-NH_2)	**42φ(ring)+**16τ(NH_2)+ 9φ(ring)+6γ(C_6H)+ 6γ (C-NH_2)
ν_4	**57(C-NH_2)+**11β(CO) +8α(ring)+8ρ(NH_2)+ 5ν(ring)	**48β(C-NH_2)+**26β(CO) +12α(ring)	**39(C-NH_2)+**24τ(NH_2) +9β(CO)+6φ(ring)	**54β(C-NH_2)+** 23β(CS)+8β(C-NH_2)	**35β(C-NH_2)+**32ν(CS) +8β(CS)+11α (ring)	**46β(C-NH_2)+**20β(CS) +12ν(CS)+5β(C-NH_2)
ν_5	26γ(N_1H)+**23φ(ring)+** 15γ(C_5H)+13φ(ring)+ 12φ(ring)+7γ(C-NH_2)	**33φ(ring)+**20γ(N1H)+ 14φ(ring)+10γ(C-NH_2) +9γ(C_5H)+8φ(ring)	**17φ(ring)+**16γ(N_1H)+ 9ω(NH_2)+9β(**C-NH_2**)+ 8τ(NH_2)+13φ(ring)+ 5ν(C-NH_2)+5γ(C_6H)	**28φ(ring)+**20γ(N_1H) +16γ(C_5H)+12φ(ring)+ 10φ(ring)+ 8γ(C-NH_2)	**35φ(ring)+**21γ(C-NH_2) +20γ(C_5H)+11φ(ring) +6φ(ring)	**25φ(ring)+**24γ(C-NH_2) +19γ(C_5H)+13φ (ring)+5γ(N_1H)
ν_6	**58τ(NH_2)+**13(CO)+ 7γ(N_1H)	48γ(C_4-N_9)+**24τ(NH_2) +**13φ(ring)+7γ(N_1H)+ 6γ(C-NH_2)	**27τ(NH_2)+**15γ(N_1H)+ 14φ(ring)+8φ(ring)+ 8γ(C_5H)+8γ(C-NH_2) +7φ(ring)	**78τ(NH_2)+**7φ(ring) +5γ(CS)	**46τ(NH_2)+**19γ(N1H)+12γ(CS) +11φ(ring) +5γ(C-NH_2)	**60τ(NH_2)+**7(C-NH_2)+ 7γ(C_6H)
ν_7	**33β(CO)+**15β(C-NH_2) + 9α(ring)+5ν(ring)	**50β(CO)+**22β(C-NH_2) +6α(ring)+5ν(ring) +5β(C-NH_2)	23γ(C-NH_2)+19ν(C-NH_2)+**11β(CO)+** 11γ(N_1H)+6ν(ring)+ 6β(C-NH_2)+ 5ν(ring)	**59β(CS)+**21β(C-NH_2)	**79β(CS)+** 7β(C-NH_2)	**49β(CS)**+18β(C-NH_2) +9γ(C_6H)+5ν(ring)
ν_8	**64α(ring)+**10β(CO)+ 6β(C-NH_2)	**76α(ring)+**6ν(ring)+ 5ν(C-NH_2)	**45α(ring)+**18β(CO)+ 11β(C-NH_2)+8α(ring)	**74α(ring)+**8ν(C-NH_2)	**74α(ring)+**6(C-NH_2) + 5α(ring)+5α(ring)	**38α(ring)+**22α(ring)+ 11ν(ring)+9γ(N_3H)
ν_9	**79α (ring)+**4α(ring)	**64α(ring)+**8ν(ring)+ 7ν(CO)+7ν(ring)	**60α(ring)+**14γ(C_6H)+ 5φ(ring)	**44α(ring)+**28ν(CS)+8β(C-NH_2)+ 5α(ring)	42β(C-NH_2)+ **21α(ring)+**18ν(CS)+ 6β(C-NH_2)+ 6β(CS)	29γ(N_1H)+**19α(ring)+** 17ν(CS) +14β(C-NH_2)
ν_{10}	**79(N_1H)+**9γ(C-NH_2) +5γ(C_5H)	**43γ(N_1H)+**18γ(C_6H)+ 17φ(ring)+12γ(CO)+ 7γ(C_5H)	**48γ(N_1H)+**10γ(C-NH_2)+ 6γ (C_5H)+5ν(C-NH_2)	**53γ(N_1H)+**24(CS)+ 14φ(ring)+6φ(ring)	**61γ(N_1H)+**16γ(C-NH_2) +9φ(ring)+6γ(CS)	**54γ(N_1H)+**15α(ring)+ 6ν(CS)+5β(CS)+ 5β(C-NH_2)+φ(ring)
ν_{11}	30γ(C-NH_2)+**30γ(C_6H) +**17γ(C_6H) +11φ(ring)	**60γ(C_5H)+**19γ(C-NH_2) +10φ(ring)	**73γ(C_5H)+**8γ(CO)+ 5γ(C-NH_2)	45φ(ring)+**18γ(C_5H)+**17γ(C-NH_2)+ 10γ(C_6H)+8γ(CS)	**60γ(C_5H)+**15γ(C-NH_2) +15γ(C_6H)+6φ(ring)	**78γ(C_5H)+**13γ(C-NH_2)
ν_{12}	36γ(C_5H)+**24γ(C-NH_2)** +11γ(CO)+9φ(ring)	31τ(NH_2)+**30γ(C-NH_2) +**15φ(ring)+8ω(NH_2)	**42γ(C-NH_2)+**25φ(ring) +8φ(ring)+ 5ν(C-NH_2)	42γ(C_5H)+**30γ(C-NH_2)** +20φ(ring)+ 5φ(ring)	55φ(ring)+**24γ(C-NH_2) +**9γ(CS)+9γ(C_6H)	**37γ(C-NH_2)+** 26φ(ring)+15γ(CS)+ 14φ(ring)
ν_{13}	**22(ring)+**10ν(ring)+ 9γ(C_5H)+8γ(CO)+ 8α(ring)+6ν(ring)+ 6ν(C-NH_2)	**53ν(ring)+**14α(ring)+ 9ν(ring)+7ν(ring)	24γ(C-NH_2)+15γ(CO) +**13ν(ring)+**7ν(ring)+ 7γ(C_5H)+ 5α(ring)	40α(ring)+**15ν(ring)+**12ν(CS)+10ν(ring)+ 5α(ring)	53α(ring)+14ν(CS)+ 9ν(ring)+6ν(ring)+ 6α(ring)	37α(ring)+**11ν(ring)+** 11ν(CS)+10ν(C-NH_2)+ 14α(ring)
ν_{14}	39φ(ring)+**37γ(CO)+** 12γ(C-NH_2)+7γ(C_5H)	**43γ(CO)+**28γ(N_1H)+ 26φ(ring)	**49γ(CO)+**28(ring)+ 5γ(C_5H)+5γ(C-NH_2)	**36γ(CS)+**23γ(C-NH_2) +15γ(N_1H)+9φ(ring)+ 5τ(NH_2)	**31γ(CS)+**17γ(N_1H)+ 15τ(NH_2)+14φ(ring)+ 9γ(C-NH_2)+ 8φ(ring)	46φ(ring)+**39γ(CS)+** 6γ(C-NH_2)
ν_{15}	**29ν(ring)+**20ν(ring)+ 12ρ(NH_2)+10α(ring)+ 7β(CO)+5ν(C-NH_2) +5β(C_6H)	**28ν(ring)+**16ν(ring)+ 11α(ring)+9ρ(NH_2)+ 7ν(CO)+6β(CO)+6ν(C-NH_2)	**34ν(ring)+**21α(ring)+8ν(C-NH_2)+7(CO) +6β(C_6H)+5α(ring)	**36ν(ring)+**13ν(ring)+13β(C-NH_2)+ 9ν(C-NH_2)+ 6α(ring)	**41ν(ring)+**9ν(CS)+ 8ν(C-NH_2)+11α(ring)	19ν(CS)+17ν(C-NH_2) +**16ν(ring)+**16α(ring)+15ν (ring)+5β(C_6H)
ν_{16}	**79(C_6H)+**13γ(C_5H)	**78γ(C_6H)+**10γ(C_5H)+ 5γ(N_1H)+ 5φ(ring)	**72γ(C_6H)+** 14φ(ring)	**80γ(C_6H)+** 12γ(C_5H)	**68(C_6H)+**24γ(C_5H)	**47γ(C_6H)+**19φ(ring)+ 10φ(ring)+7γ(N_1H)+ 5α (ring)
ν_{17}	**53α(ring)+**23ν(ring)+ 6ν(ring)	**30(ring)+**21α(ring)+ 14ν(ring)+10β(CO)+ 8ν(ring)	**42α(ring)+**22ν(ring)+6β(CO)+6 ν(ring)+5ν(ring)	**48α(ring)+**11ν(ring)+11(ring)+9ν(ring)+ 9ν(ring)	**47α(ring)+**16ν(ring) +15ν(ring)+9ν(ring)	**38α(ring)+**23ν(ring)+ 14ν(ring)+6ν(ring)
ν_{18}	**40ρ(NH_2)+17**ν(ring)+ 16β(CO)+10ν(ring)	**19ρ(NH_2)+17**ν(ring)+ 16α(ring)+12α(ring)+ 9ν(ring)+9ν(CO)	**47ρ(NH_2)+**12β(CO)+ 10ν(ring)+9ν(ring)+ 6ν(ring)+5ν(ring)	**52(NH_2)**+10ν(ring)+ 6ν(ring)+5β(CS)+ 5ν(ring)+5ν(ring)+ 5ν(CS)	**47ρ(NH_2)+**16ν(ring)+ 8α(ring)+7ν(ring)+ 5ν(CS)	**56ρ(NH_2)+**15(C_5H)+ 13ν(ring)
ν_{19}	**39β(C_5H)**+28ν(ring)+ 15ν(ring)	**36β(C_5H)+**25ν(ring)+ 15ν(ring)+7ρ(NH_2)+ 7β(N_1H)	33β(C_6H)+**27β(C_5H)+** 12β(N_1H)+10ν(ring)+ 6ν(ring)+5ν(ring)	**25β(C_5H)+**16ν(CS)+ 15ν(ring)+12ν(ring)+ 9ν(ring)+5α(ring)+ 5β(CS)	38ν(ring)+**29β(C_5H)+** 8ν(ring)+5β(C-NH_2) +5α(ring)	31ν((ring)+28ν(ring)+ **14β(C_5H)+**8ν(ring)
ν_{20}	24β(C_6H)+20ν(ring)+ **16β(N_1H)+**12β(C_5H)+ 10ν(ring)	22ν(ring)+18β(C_6H)+ 16ρ(NH_2)+15β(C_5H)+ **10β(N_1H)+** 6β(C-NH_2)	**47β(N_1H)+**11ν(ring)+ 9ν(C-NH_2)+7β(C_2H)+ 5ν(ring)+5α(ring)+ν(CO)	36β(C_6H)+20ν(ring)+ **18β(N_1H)+**15β(C_5H)	22β(C_6H)+19β(C_5H)+ 19ν(ring)+**13β(N_1H)+** 12ν(ring)+ 6ν(ring)	**21β(N_1H)+19**ν(ring)+ 19β(C_6H)+18ν(ring)+ 7β(C_5H)
ν_{21}	**42ν(ring)+**9ν(C-NH_2) +8β(C_6H)+8ν(ring)+ 7ν(ring)+5β(C-NH_2)	**22ν(ring)+**21ν(CO)+ 20ρ(NH_2)+12β(C_6H)+ 8β(N_1H)	29ν(ring)+19ν(ring)+ 18ν(ring)+9β(C_5H)+ 7ν(ring)+7β(N_1H)	41ν(ring)+10ν(ring)+ 10ν(ring)+8ν(ring)	26ν(ring)+16ν(ring)+ 11ν(ring)+8β(C-NH_2) +8ν(ring)+8β(C-NH_2)	32ν(C-NH_2)+ 24α(ring)+17β(C_5H)+ 6ν(ring)+ 5ν(CS)

ν_{22}	**23β(C_6H)+**22ν(C-NH_2) +17β(C_5H)+11ν(ring)	**19β(C_5H)+**17ν(ring)+ 15ν(C-NH_2)+15ν(ring) +9β(C_5H)+ 5ρ(NH_2)	**29β(C_5H)+**15ν(ring)+ 14β(C_6H)+14β(N_1H)+ 10ν(ring)+6ν(C-NH_2)	24ν(ring)+**22β(C_5H)+**19β(C_5H)+10ν(ring)+9α(ring)	**24β(C_6H)+**16ν(ring)+ 12β(C_5H)+10ν(ring)+ 10ν(ring)+8β(N_1H)+ 5β(C-NH_2)	**33β(C_6H)+16**β(C_5H)+ 13β(C-NH_2)+11ν(ring) +5β(C-NH_2)+5ν(ring)
ν_{23}	36β(N_1H)+**14ν(ring)+** 13ν(ring)+8ν(ring)+ 5ρ(NH_2)	**20ν(ring)+**17ν(ring)+ 12ν(CO)+10β(C_6H)+ 8ν(ring)+6ν(ring)+ 5ν(ring)+5β(C_5H)	**42ν(ring)+**16ν(ring)+ 10ν((C-NH_2)+7ν(ring) +7β(CO)	**22ν(ring)+**19β(N_1H)+17ν(ring)+9ν(ring)+ 8ρ(NH_2)+7β(C-NH_2)	**17ν(ring)+**15β(N_1H)+ 14β(C_5H)+13ν(ring)+ 10ν(ring)+10ν(ring)+ 6ν(ring)	47β(N_1H)+**17ν(ring)+** 9ν(ring)+6β(C_6H)
ν_{24}	20ν(ring)+19**ν(C-NH_2)** +17β(C_6H)+14β(C_5H)+11ν(ring)+6σ(NH_2)	31β(N_1H)+**19ν(C-NH_2)** +10ν(ring)+8σ(NH_2)+ 7ν(ring)+6ν(ring)+ 6β(C_2H)	22**ν(C-NH_2)**+15β(C_5H) +13ν(ring)+12ν(ring)+ 11β(C_6H)+ 9ν(ring)	32**ν(C-NH_2)**+ 16β(C_6H)+16ν(ring)+ 10β(C_5H)+8β(C-NH_2) + 7β(N_1H)+6ν(ring)	**26ν(C-NH_2)+**16ν(ring) +15β(C-NH_2)+ 12β(C_6H)+7β(N_1H)+ β(C_5H)	**32ν(C-NH_2)+**24α(ring) +17β(C_5H)+6ν(ring)+ 5ν(CS)+5ν(ring)
ν_{25}	**26(ring)+**21ν(ring)+ 11β(N_1H)+9ν(ring)+ 7ν(ring)+6β(C_5H)	**35ν(ring)+18**β(C_6H)+ 10β(C_5H)+9ν(ring)+ 7ν(C-NH_2)+7ν(CO)	**37ν(ring)+**18β(C-NH_2)+ 10ν(ring) +8β(C-NH_2)	24β(N_1H)+**15ν(ring)+**13ν(ring)+12ν(ring)+ 8α(ring)+7β(C_5H)+ 5ν(ring)	36β(N_1H)+**17ν(ring)+** 12ν(ring)+ 9ν(ring)	**43ν(ring)+**9ν(ring)+ 7β(C_5H)+6ν(ring)+ 6β(N_1H)
ν_{26}	**79σ(NH_2)+11**ν(C-NH_2) + 5ν(ring)	**54σ(NH_2)+**30ν(C-NH_2)	**90σ(NH_2)**	**71σ(NH_2)**+12ν(C-NH_2) + 6ν(ring)	**46σ(NH_2)**+21ν(ring)+ 10ν(C-NH_2)+ 7ν(ring)	**92σ(NH_2)**
ν_{27}	**39ν(ring)+**13ν(ring)+ 11β(C_6H)+9ν(ring)+ 7α(ring)+5ν(C-NH_2)	**26ν(ring)+**22σ(NH_2)+ 9β(C_6H)+8β(C_5H)+ 6ν(CO)+6β(N_1H)+ 5ν(ring)+5α(ring)	**38ν(ring)+**21β(C_6H)+ 10ν(ring)+8ν(ring)+ 7α(ring)	**39ν(ring)+**10ν(ring)+10β(C_6H)+8α(ring)+ 8ν(ring)+7ν(ring)	**25ν(ring)+**20β(C-NH_2) +19ν(ring)+ 7α(ring)	**28ν(ring)+**13β(C_5H)+ 13β(C_6H)+11α(ring)+ 10ν(ring)+7ν(ring)
ν_{28}	**72(CO)+**9ν(ring)+ 5α(ring)	**34ν(CO)+**16β(N_1H)+ 9ν(ring)+8ν(ring)+ 6ν(ring)	**68ν(CO)+**11ν(ring)+ 6β(N_1H) +5α(ring)	29ν(ring)+**16ν(CS)+** 10β(C_5H)+9α(ring)+ 8β(N_1H) +8ν(ring)	35ν(ring)**+16ν(CS)+** 13α(ring)+12β(C_6H)+ 5β(N_1H)	27ν(ring)+**19ν(CS)+** 16α(ring)+8β(CS)+ 6β(C_5H)+6ν(ring)
ν_{29}	**86ν(C_6H)+** 13(C_5H)	**62ν(C_6H)+**38ν(C_5H)	**98ν(C_5H)**	**80ν(C_6H)+** 19ν(C_5H)	**73ν(C_6H)+** 26ν(C_5H)	**94ν(C_6H)+** 6ν(C_5H)
ν_{30}	**87ν(C_5H)+**12(C_6H)	**62ν(C_5H)+** 37ν(C_6H)	**98ν(C_5H)**	**81ν(C_5H)+18**ν(C_6H)	**73ν(C_5H)+** 26ν(C_6H)	**93ν(C_5H)+** 6ν(C_6H)
ν_{31}	**62(N_9H_{12}) +37ν(N_9H_{13})**	**64ν(N_9H_{12})+34ν(N_9H_{13})**	**74ν(N_9H_{13})+ 26ν(N_9H_{12})**	**57ν(N_9H_{12})+31ν(N_9H_{13}) +11ν(N_1H)**	**57ν(N_9H_{12})+ 34ν(N_9H_{13})+8ν(N_1H)**	**60ν(N_9H_{12})+ 40ν(N_9H_{13})**
ν_{32}	**99ν(N_1H)**	**98ν(N_1H)**	**100ν(N_1H)**	**88ν(N_1H)+7**ν(N_9H_{12})	**91ν(N_1H)**	**100ν(N_1H)**
ν_{33}	**63ν(N_9H_{13})+ 37ν(N_9H_{12})**	**65ν(N_9H_{13})+ 35(N_9H_{12})**	**75ν(N_9H_{12})+ 25ν(N_9H_{13})**	**64ν(N_9H_{13})+ 35ν(N_9H_{12})**	**62ν(N_9H_{12})+ 38ν(N_9H_{13})**	**61ν(N_9H_{13})+ 39ν(N_9H_{12})**

$ Same as in Table- 3

Table 4: PEDs (Potential Energy Distributions)[$] of Cytosine, Thiocytosine and their cations and anions.

ν_5, ν_3 and ν_1; the mode ν_5 is calculated to be 395/404 cm^{-1} for the Cyt/TCyt molecules. This mode (ν_5) was earlier assigned at 421(IR) and 400 cm^{-1} (R) for Cyt [9] and 422 (IR) and 423(R) cm^{-1} for TCyt [11]; the mode (ν_3) has calculated frequency 200 for Cyt and 185 cm^{-1} for TCyt molecule. The lowest ring deformation mode ν_1 is calculated to be 128 and 111 cm^{-1} for the Cyt and TCyt molecules respectively and it could be observed in the Raman spectrum at 123 cm^{-1} for Cyt [9] and at 98 cm^{-1} for TCyt [11].

C-H/N-H modes: The ν (NH) mode (ν_{32}) is calculated to have frequencies 3618 and 3600 cm^{-1} for Cyt and TCyt molecules respectively. The NH stretching mode is coupled with the symmetric stretching of the NH_2 group in the out-of-phase (opc) manner for TCyt molecule. The NH bending mode ν_{20} is calculated to be 1214 and 1231 cm^{-1} for the Cyt and TCyt molecules and it could be correlated to the frequencies 1235(IR) and 1249 cm^{-1} (R) for TCyt [11]. The NH out-of-plane bending mode (ν_{10}) is calculated to be 619 and 658 cm^{-1} for the Cyt and TCyt molecules and this mode is found to be depolarized in case of the TCyt molecule. The bands for the ν_{10} mode were observed at 600 cm^{-1} (IR)/597cm^{-1} (R) for the Cyt and at 652 cm^{-1} (IR)/659 cm^{-1} (R) for the TCyt molecule [11].

In the Cyt molecule, the C_5-H out-of-plane bending mode (ν_{11}) is in in-phase coupling (ipc) with N-H and the C_6-H out-of-plane bending mode (ν_{16}) is coupled with C_5-H in opc manner. In the neutral molecules, the two C-H stretching modes are ν_{30} and ν_{29} the higher frequency mode is ipc stretching mode whereas the lower frequency corresponds to the opc stretching mode due to C_5H and C_6H. Susi et al. [9] have observed the frequencies at 3169 (IR) and 3176 (R) cm^{-1} for the Cyt molecule and Yadav et al. [11] observed bands 3063 and 3061 cm^{-1} in the IR and Raman spectra of the TCyt molecule for the CH stretching mode (ν_{30}). The CH stretching mode (ν_{29}) was observed for Cyt by Susi et al. [9] only in Raman spectrum at 3230 cm^{-1} and the IR/Raman frequencies observed at 3094/3090 cm^{-1} for the TCyt molecule [11] which correspond to this mode.

The C_6-H and C_5-H in-plane bending modes ($\nu_{22,}$ ν_{19}) have been calculated to be 1354/1125 cm^{-1} for the Cyt molecule and 1371/1109 cm^{-1} for the TCyt molecule. The IR intensity and Raman activity decreases slightly for ν_{22} but IR intensity of the mode ν_{19} increases by a factor of ~ 33 in going from Cyt to TCyt. The observed frequencies for the mode ν_{22} could be assigned at frequency 1364 and 1361 cm^{-1} in IR and Raman spectra for Cyt [9] and it could be assigned at the 1368 and 1370 cm^{-1} in the IR and Raman frequencies for TCyt [11]. The mode ν_{19} could be assigned at the observed frequencies 1100 (IR) and 1108 (R) cm^{-1} for Cyt which was earlier assigned by Susi et al. [9] as a ν(ring) mode. The observed frequencies 1098 (IR) and 1104 (R) cm^{-1} were assigned to the (NH_2) mode by Yadav et al. [11] which is reassigned to the β(C_5H) mode for TCyt.

The two out-of-plane CH bending modes ν_{16} and ν_{11} are found to be 957 and 723 cm^{-1} for the Cyt molecule. However, the observed frequencies 701(IR)/723 (R) cm^{-1} correspond to the mode ν_{11} and 966 (IR)/971 (R) cm^{-1} to the mode ν_{16} for the Cyt molecule [9]. The CH out-of-plane bending modes for TCyt are calculated to be 960 and 730 cm^{-1}. The mode ν_{16} could be correlated to the observed frequencies 967 (IR)/965 (R) cm^{-1} and the frequencies 724 (IR)/718 (R) cm^{-1}, which were earlier assigned to the ring stretching mode, could be reassigned to the mode ν_{11} [11] for the TCyt molecule.

C=O/S modes: The C=O stretching mode for Cyt is calculated to

be 1769 cm^{-1} and the ν(C=S) mode to be 1142 cm^{-1}. The ν (C=S) mode could be correlated to the IR/Raman frequencies at 1163/1167 cm^{-1} which were observed and assigned earlier to one of the ν (ring) modes [11]. The C=O/S bending modes for the Cyt and TCyt molecules are calculated to be 533 and 269 cm^{-1}, whereas, the γ (C=O/S) for Cyt and TCyt are calculated to be 774 and 651 cm^{-1} respectively. The observed frequencies 533 (IR) and 533 (R) were assigned to the β (C=O/S) modes for the Cyt molecule [9].

C-NH_2 modes: The calculated frequency for the ν(C-NH_2) mode found to be 1499 / 1496 cm^{-1} for the neutral Cyt/TCyt molecules with the enhanced IR intensity by a factor of ~ 2 in going from Cyt to TCyt. The observed frequencies 1505 (IR)/1498 (R) cm^{-1} could be correlated to this mode for Cyt which were earlier assigned to ν(ring) mode by Susi et al. [9]. The above mode was assigned at 1504 and 1495 cm^{-1} from the IR and Raman spectra of TCyt by Yadav et al. [11]. The bending mode of the C-NH_2 group (ν_4) is calculated to be 358 cm^{-1} for Cyt and 438 cm^{-1} for TCyt. It can also be seen from the Table 3 that the magnitude of this mode increases by 80 cm^{-1} in going from Cyt to TCyt. Yadav et al. [11] assigned this mode at 434 and 432 cm^{-1} based on the IR and Raman spectra. The frequencies 760 (IR) and 764 cm^{-1} (R) for Cyt [9] could be assigned to the out-of-plane bending mode of C-NH_2 (ν_{12}). The γ (C-NH_2) mode could be correlated to the 752 and 755 cm^{-1} in IR and Raman bands which were assigned earlier to the γ (N_1H) mode [11].

NH_2 modes: The symmetric and anti-symmetric stretching modes (ν_{33}, ν_{31}) of the amino group (NH_2) have characteristic magnitudes in the range 3200-3500 cm^{-1}. For the TCyt molecule we have assigned the frequency 3334 cm^{-1} observed in IR/Raman spectra to the anti-symmetric stretching mode (ν_{33}) while the symmetric stretching mode (ν_{31}) was observed at 3312 (IR)/3320 (R) cm^{-1} [11]. The (ν_{31}) mode was observed by Susi et al. [9] at 3380 (IR)/3354 (R) cm^{-1} for Cyt. The Raman activities for symmetric and anti-symmetric stretching modes of NH_2 are increased by factors of ~2 and ~9 in TCyt than those in the Cyt molecule. The anti-symmetric stretching mode (ν_{33}) of NH_2 group is a pure mode but the symmetric mode (ν_{31}) of the NH_2 group is ipc with the stretching mode (ν_{32}) of the N_1H bond in the TCyt molecule. The NH_2 scissoring mode (ν_{26}) of Cyt/TCyt is calculated to be 1632/1636 cm^{-1}. The IR intensity and Raman activity decrease by the same factor of ~ 2 in TCyt as compared to Cyt. This mode was observed at 1615 (IR) and 1612 (R) cm^{-1} by Susi et al. [9] and 1630 cm^{-1} (R) by Yadav et al. [11]. The ρ (NH_2) mode (ν_{18}) is calculated to be 1084/1069 cm^{-1} for the Cyt/TCyt molecules and for TCyt this mode is found to shift downward than that in Cyt. The calculated frequency for the τ(NH_2) is found to be 525 and 538 cm^{-1} for the Cyt and TCyt molecules respectively. In the Cyt molecule torsion mode (ν_6) could be assigned at 520 (IR) and 517 (Raman) cm^{-1} [9] while in TCyt it was observed at 527 cm^{-1} in the IR spectrum [11]. The wagging mode of the NH_2 group (ν_2) for TCyt (50 cm^{-1}) is calculated to be at much lower frequency than that in Cyt (180 cm^{-1}). The frequency for (NH_2) has been observed at 162 cm^{-1} for the Cyt molecule [9] and at 50 cm^{-1} for the TCyt molecule [11] in the Raman spectra.

Radical cations: In the following discussion only those modes have been discussed for which the frequencies change significantly upon the cationic radicalization.

Ring modes: It is to be noticed that the frequency corresponding to the breathing mode ν_{13} decreases by 45 cm^{-1} with increases in the IR intensity and Raman activity in going from Cyt to Cyt^+. In case of the TCyt molecule no change is found in the frequency due to removal of one electron while the IR intensity increases in $TCyt^+$ as compared to TCyt. The intensity of the IR band for mode ν_{15} decreases by a factor of ~ 2 while Raman activity increases by a factor of ~ 18 and the depolarization ratio is also increased in going from Cyt to Cyt^+. In going from TCyt to $TCyt^+$ the IR intensity decreases by a factor of ~ 10 while Raman activity increases by a factor of ~ 8. The radicalizations of Cyt and TCyt into their radical cations increase the frequency of mode ν_{21} by 111 and 179 cm^{-1} respectively. Due to the radicalization process, the ν_{21} mode is found to decrease by 78 cm^{-1} with considerably increased IR intensity, Raman activity and depolarization ratio in the Cyt^+ as compared to that of the Cyt, whereas it is found to increase by 179 cm^{-1} with decreased IR intensity/Raman activity by factors ~ 1/3 / ~ 1/8 in $TCyt^+$ as compared to that of TCyt. The mode ν_{23} is increased by 47 cm^{-1} in Cyt^+ with slight decrease in IR intensity and increase in Raman activity. For the mode ν_{23} the frequency decreases by 45 cm^{-1} in going from TCyt to $TCyt^+$ with decrease in the IR intensity and Raman activity. In the radicalization process for the mode ν_{25} IR intensity decreases but the Raman band becomes stronger and depolarized in going from Cyt to Cyt^+. In going from TCyt to $TCyt^+$ the frequency of this mode increases by 25 cm^{-1}, the depolarization ratio increases by a factor of ~ 6. In the present calculation the frequency of the mode ν_{27} is shifted upward by 74 cm^{-1} in Cyt^+ compared to that for the Cyt molecule. Moreover, the IR intensity of the ring stretching mode ν_{27} decreases by a factor of ~ 4 and Raman activity increases by a factor of ~ 4 in the cationic radicalization process of Cyt and slight increment in frequency is noticed for $TCyt^+$ as compared to that of the TCyt molecule. In going from Cyt to Cyt^+ the Raman activity increases by a factor of ~ 20 for the in-plane ring deformation mode (ν_8) and in going from TCyt to $TCyt^+$ the Raman activity increases two fold. The frequency of the mode ν_9 is found to decrease by ~ 34 cm^{-1} in $TCyt^+$ than that of TCyt. The IR intensity increases by a factor of ~ 6 for Cyt^+ but in case of $TCyt^+$ the IR intensity and Raman activity decrease by factors of ~ 1/6 and ~ 1/17 respectively for the mode ν_9. The magnitude of frequency of the planar-ring deformation mode ν_{17} for Cyt decreases by 39 cm^{-1} while the other vibrational parameters increase considerably due to the radicalization process. In case of Cyt^+ the Raman band becomes polarized and in going from TCyt to $TCyt^+$, the IR intensity decreases by factor of ~ 1/12 for this mode.

The frequency of the non-planar ring deformation mode ν_1 shifts towards lower wavenumber side by 30 cm^{-1} and IR intensity increases by a factor of ~ 5 for Cyt^+. In the case of $TCyt^+$, the calculated frequency is found to increase by 36 cm^{-1} and the Raman band is depolarized. For the mode ν_5, the IR intensity decreases by a factor of ~ 1/4 in going from Cyt to Cyt^+ and the Raman band changed from depolarized to polarize in $TCyt^+$. Due to removal of an electron, the ν_3 mode is found to decrease by 80 cm^{-1} for $TCyt^+$ as compared to the neutral molecule and the Raman band is found to be depolarized while the IR intensity decreases in Cyt^+ as compared to Cyt.

C-H/N-H modes: Out of the two C-H stretching modes (ν_{30}, ν_{29}) the higher frequency (ν_{30}) has been assigned to the C_5-H stretching which is opc with the C_6-H stretching and the lower stretching mode (ν_{30}) has been assigned to the stretching mode of C_6-H which is also strongly coupled with the C_5-H stretching in ipc manner. For the ν_{30} mode the IR intensity increases by a factor of ~ 4 and Raman activity decreases by a factor of ~ 1/3 with increase of the depolarization ratio for $TCyt^+$ than that of TCyt. The magnitude of the mode ν_{29} shifts towards higher frequency by 30 cm^{-1} and IR intensity/Raman activity increases by a factor of ~ 4/2 but depolarization ratios are decreased in going from TCyt to $TCyt^+$. Assignments for in – plane bending modes of C-H (ν_{20}, ν_{19}) are relatively complicated due to mode mixing. The in-plane C-H bending modes are strongly coupled with the ring stretching mode. Due to removal of one electron from the neutral molecules Cyt

and TCyt, in Cyt^+ radical the IR intensity decreases by a factor of ~ 1/4 while the Raman activity increases by a factor of ~ 4 with increases in depolarized ratio than that of Cyt for the mode ν_{19}. The IR intensity of above mode is decreased by a factor of ~ 1/10 but the Raman activity increases by a factor of ~ 3 with decrease in depolarization ratio in $TCyt^+$ compared to TCyt. The mode ν_{20} (in-plan bending mode of C_6H) in Cyt^+ shifts towards the lower frequency by 97 cm^{-1} and Raman activity increases drastically. The depolarization ratio for this mode is increased in both the Cyt^+ and $TCyt^+$ species than the corresponding neutral molecule.

Out-of-plane C-H bending mode (ν_{16}) shifts towards higher frequency by 34 cm^{-1} in going from Cyt to Cyt^+. The calculated frequency of the mode ν_{11} for Cyt^+/ Cyt^+ increases by 122/93 cm^{-1} than those in Cyt/TCyt. For the above mode the IR intensity in Cyt^+ is decreases by a factor of ~ 3 and Raman band becomes depolarized while the IR intensity and Raman activity increase with decrease depolarization ratio in $TCyt^+$ as compared to TCyt.

The N-H stretching frequency (ν_{32}) shifts towards lower wavenumber by 82 cm^{-1} and the IR intensity increases by a factor of ~5 but Raman activity decreases by a factor of ~ 2 in Cyt^+ as compared to the Cyt molecule. However, in $TCyt^+$ the IR intensity is noticed to be weaker and the Raman activity increases by a factor of ~ 10 than that of TCyt. The N-H stretching mode is coupled with the symmetric stretching mode of the NH_2 group in ipc manner for $TCyt^+$. The in-plane N-H bending mode (ν_{22}) is increased by 151 cm^{-1} and Raman activity increases by a factor of ~ 4 for Cyt^+ than that of Cyt. The in-plane N-H bending mode is strongly coupled with both the C-H in-plane bending modes in ipc manner. The mode ν_{10} is defined as the out-of-plane N-H deformation mode which is found to increase by 89 cm^{-1} and have depolarized Raman band in Cyt^+ as compared to the Cyt molecule. However, the frequency of the above mode (ν_{22}) is found to decrease by 103 cm^{-1} with increase in Raman activity by a factor of ~ 15 and Raman band becomes polarized in $TCyt^+$ than that in TCyt molecule.

C=O/S Modes: A drastic change is found for the C=O stretching mode ν_{28} which is decreased by 343 cm^{-1} in Cyt^+ but ν(C=S) increases by 63 cm^{-1} in $TCyt^+$. The IR intensity decreases while the Raman activity increases in Cyt^+ than those in neutral molecule and in case of $TCyt^+$ the IR intensity is decreased than that of TCyt molecule. For the in-plane bending mode of (C=O/S) (ν_7) for Cyt^+ Raman activity increases by a factor ~ 23 with depolarized Raman band. In the $TCyt^+$ species the frequency decreases by 56 cm^{-1} and Raman band becomes depolarized for the mode ν_7. The frequency of the C=O/S out-of-plane bending mode (ν_{14}) decreases by 37 cm^{-1} in Cyt^+ and by 26 cm^{-1} in $TCyt^+$ due to removal of one electron. The Raman band is depolarized in Cyt^+ and IR intensity decreases by a factor of ~ 1/7 in $TCyt^+$ for ν_{14} mode.

C-NH_2 modes: The mode ν_{24} increases by 45 cm^{-1} in $TCyt^+$ with decreased in IR intensity by a factor of ~1/2 and depolarization ratio increases. The frequency of C-NH_2 in-plane bending mode ν_4 is found to slightly decrease in Cyt^+ but the IR intensity/Raman activity increase. In $TCyt^+$ the IR intensity and Raman activity increase by a factor of ~ 2 but the polarizability of Raman band decreases than that of TCyt. The mode ν_{12} is found to decrease by 207 cm^{-1} and IR intensity increases by a factor of ~ 4 while the polarizability of this band changes from polarized to depolarize in going from Cyt to Cyt^+. The IR intensity and depolarization ratio decrease in going from TCyt to $TCyt^+$ for this mode.

NH_2 modes: The anti-symmetric stretching mode of NH_2 group (ν_{33}) decreases by ~ 45 and ~ 46 cm^{-1} in Cyt^+ and $TCyt^+$ than those of neutral molecules respectively. For ν_{33} modes the IR intensity and Raman activity increase 2-fold for Cyt^+ while in case of $TCyt^+$ only the IR intensity increases by a factor of ~2. For the symmetric stretching mode of NH_2 (ν_{31}), the decrease is noticed by ~ 37 cm^{-1} while the IR intensity and Raman activity increase 2-fold for Cyt^+. In case of $TCyt^+$ the IR intensity increases by a factor of ~ 7 while the Raman activity decreases by a factor of ~ 1/3 for $TCyt^+$ as compared to the neutral molecule TCyt. The anti-symmetric stretching mode of NH_2 is a pure mode in $TCyt^+$ but the symmetric mode of NH_2 mode is opc with the stretching of N-H in $TCyt^+$.

The frequency of scissoring mode of NH_2 group (ν_{26}) increases by 47 cm^{-1} and IR intensity and Raman activity also increase by factors ~ 3 and ~ 2 for Cyt^+ species than that of Cyt. In case of the $TCyt^+$ species the ν_{26} mode is increased by 29 cm^{-1} with decrease in IR intensity but an increase is noticed in the Raman activity by a factor of ~ 3 as compared to TCyt. The frequency of the rocking mode (ν_{18}) of the amino group for Cyt^+ decreases by 85 cm^{-1} with increase in IR intensity by a factor of ~2 while the Raman activity increases drastically. In $TCyt^+$ the IR intensity and Raman activity are decreased by factors of ~ 1/3 and ~ 1/4 respectively while the depolarization ratio increases.

The torsion mode of NH_2 (ν_6) increases by 116 cm^{-1} in Cyt^+ and 56 cm^{-1} in $TCyt^+$ respectively and Raman band becomes depolarized in case of Cyt^+ species. The increase of IR intensity by factors of ~ 4 / ~ 10 in Cyt^+/$TCyt^+$ species for the (ν_6) mode. The calculated frequencies of the wagging mode of NH_2 group (ν_2) are found to be 477 cm^{-1} and 500 cm^{-1} in Cyt^+ and $TCyt^+$ respectively, while the frequency for this mode increases drastically by 297 and 450 cm^{-1} than that of the neutral Cyt and TCyt molecules. The polarization of the Raman band changes from the polarized to depolarize in Cyt^+ species while the polarization ratio increases in $TCyt^+$.

Radical anion: Due to the addition of one electron to the neutral Cyt and TCyt molecules most of the vibrational characteristics change as compared to their neutral Cyt and TCyt molecules. The following discussions are made only for those modes which show major differences as compared to the neutral molecules.

Ring modes: The IR intensities and Raman activities of the calculated vibrational frequencies for all the ring modes increase in Cyt^- than those in Cyt. The calculated vibrational frequencies of ring stretching modes ((ν_{21}, ν_{25} and ν_{27}) are decreased by 285, 187 and 129 cm^{-1} for Cyt^- than those in neutral Cyt molecule, whereas, for TCyt the mode ν_{27} is decreased by 218 cm^{-1} but the mode ν_{23} is increased by 34 cm^{-1} for TCyt radical than those in neutral TCyt molecule. During the ring stretching vibrations the ring angles also change periodically so that the hexagonal shape of the ring gets distorted. The in-plane ring deformation modes (ν_9, ν_{13}, ν_{17}) are unchanged due to attachment of one electron to the Cyt molecule. In going from Cyt to Cyt^- the IR intensities and Raman activities increased drastically for above modes. The frequency shifts downward by 18 cm^{-1} and the IR intensity increases by a factor of ~ 4 for the in-plane ring deformation mode (ν_9) in the $TCyt^-$ radical. In going from TCyt to its anion IR intensity decreases by a factor of ~ 1/5 while Raman activity increases by a factor of ~ 10 for the mode ν_{17}. An increment is noticed for the IR intensity, Raman activity and depolarization ratio increase for the ν_{13} mode in $TCyt^-$ as compared to TCyt. The vibrational frequencies of the non-planar deformation modes of the ring (ν_5) is found to decrease by 83 cm^{-1} for Cyt^- and 99/211 cm^{-1} for the modes ν_5/ ν_3 in the $TCyt^-$ species. The IR intensities and Raman activities are increased drastically while the polarization change from depolarized to polarized for all the out-of-

plane deformation modes (ν_1, ν_3 and ν_5) in going from neutral to anions of Cyt and TCyt.

C-H/N-H Modes: The N-H stretching mode (ν_{32}) is a pure mode and decreases by 37 cm^{-1} for $TCyt^-$ than that of TCyt molecule and IR intensity decreases by a factor of ~ 1/6 while Raman activity increases drastically. The mode (ν_{30}) is decreased with equal magnitudes by 69 cm^{-1} for both the radicals Cyt^- and $TCyt^-$. As a result of anionic radicalization in going from neutral to anions of Cyt and TCyt their vibrational parameters are found to increase for the modes (ν_{29}, ν_{30}). The lower stretching frequency defined as stretching mode of C_5-H, is very slightly coupled with C_6-H stretching in opc manner in anionic radicals of Cyt and TCyt. The stretching mode of C_6-H is strongly coupled with the C_5-H in ipc manner for the $TCyt^-$ radicals. The mode ν_{19}/ν_{22} are increased by 46/66 cm^{-1} for Cyt^- as compared to the neutral Cyt molecule and the calculated frequency for in-plane bending mode of N_1-H (ν_{20}) for Cyt^- increases by 214 cm^{-1}. In case of Cyt^- the IR intensities and Raman activities are found to increase due to attachment of electron to its neutral molecule. For the anionic Cyt radical, the in-plane bending mode of C_6-H is in opc with C_5-H and N_1-H while the in-plane bending mode of C_5-H is in opc only with N_1-H. The ν_{19} and ν_{22} are decreased by 122 and 45 cm^{-1} for $TCyt^-$ species with increased polarizability of Raman band than those of TCyt molecule. In going from TCyt to $TCyt^-$ the IR intensities for the modes ν_{19} and ν_{22} are decreased by factors of ~ 1/2 and 1/15 while it is increased 2-fold for the mode ν_{20}. During the above two C-H in-plane bending modes (ν_{19} and ν_{22}) of vibration for each of the two molecules the H atoms vibrate in the same phase in higher magnitude and out-of-phase in lower magnitude mode. The out-of-plane bending modes of the two C-H and one N-H bonds are denoted as ν_{16}, ν_{11} and ν_{10} in which the out-of-plane bending mode of C_6-H (ν_{16}) is ipc with N_1-H and out-of-plane bending mode of C_5-H (ν_{11}) is in opc with C_6-H while the out-of-plane bending mode of N_1-H (ν_{10}) is slightly coupled in opc with C_6-H for both the anions Cyt and TCyt. The mode ν_{16} is decreased by 362/646 cm^{-1} while the mode ν_{11} is increased by 79/28 cm^{-1} in Cyt^-/$TCyt^-$ than those in Cyt and TCyt respectively. A decrease is also found by 129 cm^{-1} in Cyt and 194 cm^{-1} in TCyt for the mode ν_{10} upon the anionic radicalization. For all these three modes the IR intensity and Raman activity are found to be increased in both Cyt and TCyt species and the change in polarization from the depolarized to polarize only in going from TCyt to $TCyt^-$.

C=O/S modes: It is found that the stretching frequency of C=O/S (ν_{28}) in Cyt and TCyt molecules are found to shift downward by 101 and 79 cm^{-1} for Cyt^- and $TCyt^-$ respectively. The IR intensity decreases and Raman activity increases for this mode in going from neutral to anions of Cyt and TCyt. The in-plane bending mode of C=O/S (ν_7) and out-of-plane bending mode of C=O/S (ν_{14}) for Cyt^- and $TCyt^-$ are found to slightly change in the magnitudes. For the above two modes IR intensities and Raman activities are increased for Cyt^- and $TCyt^-$ while Raman bands become polarized only for $TCyt^-$.

C-NH_2 modes: The present calculation shows that the frequency of the stretching modes of C-NH_2 (ν_{24}) for Cyt^- species are lowered by 193 with increase in IR intensity by a factor of ~ 7 and out-of-plane bending (ν_{12}) shifts downward by 107 cm^{-1} with increase in Raman activities for both the modes than the neutral Cyt molecule. Due to attachment of electron to the neutral Cyt depolarization ratios decrease for ν_{24} and ν_4 while it increases for the $_3$ mode. The modes ν_{24} and ν_{12} for $TCyt^-$ species are lowered by 233 and 39 cm^{-1} than its neutral TCyt. It is also noticed that the IR intensity decreases by a factor of ~ 1/8 and Raman activity increases by a factor of ~ 16 for the mode ν_{24} while both properties are increased 2-fold for the mode ν_4 in going from TCyt to $TCyt^-$. The out-of-plane bending mode of C-NH_2 is ipc with C_6-H and opc with N_1H and C_5-H for the Cyt^- radical. However, the in-plane bending mode of C-NH_2 (ν_{24}) is found to be equal in the magnitude of the calculated vibrational frequency for Cyt^- and $TCyt^-$.

NH_2 modes: In the case of anionic radicalization of Cyt and TCyt molecules, the (ν_{31} and ν_{33}) are found to shift downward by 195/130 cm^{-1} and 178/152 cm^{-1} with increase in IR intensity and Raman activity in Cyt^-/$TCyt^-$ as compared to their neutral molecules. The calculated vibrational frequencies for the modes ν_{26} and ν_6 are decreased by 43 and 196 cm^{-1} while for the mode ν_2 it is increased by 375 cm^{-1} in Cyt^- than those in Cyt. In case of $TCyt^-$ species, the modes ν_{18}, ν_6 and ν_2 are increased by 52, 333 and 753 cm^{-1} as compared to the TCyt molecule. It is found that the IR intensities and Raman activities for all the modes are increased drastically due to attachment of one electron on the neutral molecules of Cyt and TCyt.

HOMO-LUMO analysis

The highest occupied molecular orbital (HOMO) and lowest unoccupied molecular orbital (LUMO) are the main orbitals that take part in chemical stability [36,37]. They are the key parameters in determining molecular properties and molecular electrical transport properties [38,39]. The eigenvalue of HOMO characterizes the ability of donating electron and the eigenvalue of LUMO characterizes the ability of accepting electrons. The energy gap between HOMO and LUMO reflects the chemical stability and they are responsible for chemical and spectroscopic properties of the molecule [40,41]. The orbitals HOMO - LUMO and their properties such as their energy are very useful for physicists and chemists. This is also used by the frontier electron density for predicting the most reactive position in π -electron system and also explains several type of reaction in conjugated system [42]. In conjugated molecules there is a small separation between HOMO-LUMO which is the result of a significant degree of intermolecular charge transfer from the end-capping electron donor groups to the efficient ele1ctron acceptor groups through π-conjugated path [43]. Energy difference between the HOMO and LUMO orbitals is called energy gap which is important for stability of structures [44]. An electronic system with larger HOMO-LUMO gap is less reactive than one having smaller gap [45]. If energy gap is larger, kinetic stability will be greater and chemical reactivity will be lower because it is energetically unfavourable to add electrons to a high lying HOMO and to remove electrons from a low lying LUMO and hence, to form an activated complex of any potential reaction [46].

The sketch of the atomic orbital compositions of the frontier MOs are shown in Figure 6. The green and red solid regions in Figure 6 represent the MOs with completely opposite phases. The present calculations predict that the energies of HOMO/LUMO orbitals of the Cyt and TCyt are -1.3665/-6.6628 eV and -1.6538/-6.6600 eV, respectively. The energy gap (ΔE), i.e. the transition energy from HOMO to LUMO of the Cyt and TCyt are 5.2963 eV and 5.0062 eV, respectively.

Molecular electrostatic potential and electrostatic potential

Molecular electrostatic potential (MEP) and electrostatic potential are correlated with the dipole moment, electronegativity, partial charges and site of chemical reactivity of the molecule. MEP provides a visual method to understand the relative polarity of a molecule. While the negative electrostatic potential corresponds to an attraction of the proton by the concentrated electron density in the molecule (and is colored in shades of red on the ESP surface), the positive electrostatic potential corresponds to repulsion of the proton by atomic nuclei in

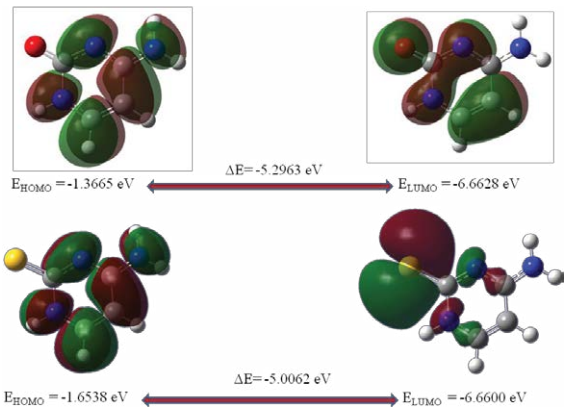

Figure 6: HOMO-LUMO energy gap for Cyt and TCyt.

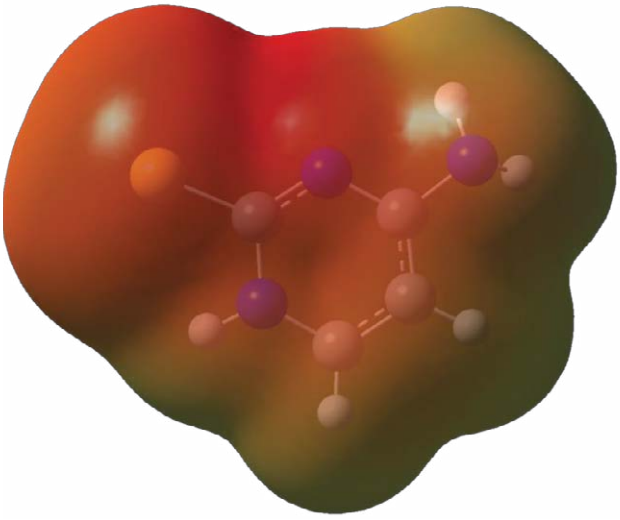

Figure 7: Molecular electrostatic potential surface of cytosine.

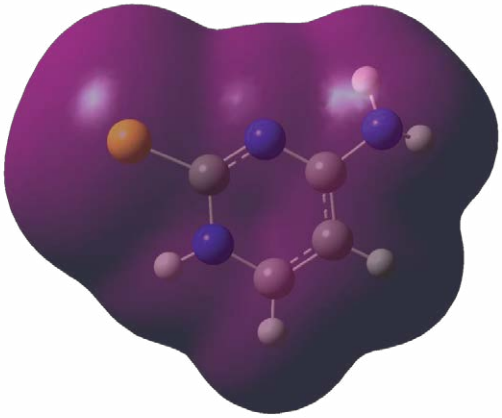

Figure 8: Electron density plot of cytosine.

regions where low electron density exists and the nuclear charge is incompletely shielded (and is colored in shades of blue). By definition, electron density isosurface is a surface on which molecule's electron density has a particular value and that encloses a specified fraction of the molecule's electron probability density. The electrostatic potential at different points on the electron density isosurface is shown by coloring the isosurface with contours. The graphical representation of the molecular electrostatic potential surface, as described by Politzer and Truhlar [47] is a series of values representing the evaluation of the interaction energy between a positively charged (proton) probe and points on a solvent accessible surface as defined by Connolly [48-51]. The electron density isosurface onto which the electrostatic potential surface has been mapped is shown in Figure 5-8. Such surfaces depict the size, shape, charge density and site of chemical reactivity of the molecules. The different values of the electrostatic potential at the surface are represented by different colors; red represents regions of most negative electrostatic potential, blue represents regions of most positive electrostatic potential and green represents regions of zero potential. Potential increases in the order red <orange<yellow<green<blue. From the MEP surface (Figure 7), it is clear that the site close to sulfur shows region of most negative electrostatic potential. The ED plot for molecule shows a uniform distribution (Figure 8).

Conclusion

The optimized geometric parameters were seen to be in good agreement with the experimental data. Cationic and anionic radicals of the Cyt and TCyt molecules are found to be stable at B3LYP/6-311++G** level. Enhancements in the bond angles N_1-C_2-N_3/C_4-C_5-C_6 are found by 1.2^0 for Cyt^- and $3.1^0/2.7^0$ for $TCyt^-$ as the anionic radicalization process. The dihedral angles C_5-C_4-N_9-H_{12}/N_3-C_4-N_9-H_{13} have values 174.3°/-170.3° suggesting that the two H-atoms of the NH_2 group are not lying in the ring plane. It is interesting to note that the bond length C_5-C_6 increases due to loss of its double bond character in Cyt^+/$TCyt^-$ and lengthens by 0.031 Å/0.047 Å in Cyt^+/$TCyt^-$ as a result of radicalization. In going from Cyt/TCyt to Cyt^+/$TCyt^+$ the electronic charge is removed mainly from the sites N_1, N_3, C_5 and O/S. The elongation of the bond lengths of C_2=O/S are noted in cationic species of Cyt/TCyt. Due to attachment of an electron to the neutral molecules Cyt/TCyt the electronic charge goes mainly to the N_1, N_3, C_5, O and all H sites in Cyt^- while in going from TCyt to $TCyt^-$ the electronic charge goes mainly to the C_2, C_4, C_6, S and all H sites.

The wagging mode of the NH_2 group for TCyt is found at much lower frequency 50 cm^{-1} than that in Cyt (130 cm^{-1}). Assignments for the C-H in - plane bending modes (ν_{22}, ν_{19}) are complicated for the ionic species due to strong coupling with the ring stretching modes. The out-of-plane deformation mode of C_6-H is strongly coupled with C_5-H in opc manner for TCyt and in ipc manner for the $TCyt^+$ and $TCyt^-$ radicals. The frequency of C=O stretching mode (ν_{28}) is found to be drastically reduced (by 343 cm^{-1}) for Cyt^+ but ν(C=S) increases by 63 cm^{-1} in $TCyt^+$. The wagging mode of NH_2 group (ν_2) is found to be increase drastically (by 297/450 cm^{-1}) as compared to those of neutral Cyt and TCyt molecules. The three in-plane ring deformation modes (ν_9, ν_{13}, ν_{17}) are found to be unchanged due to attachment of an electron to the Cyt molecule. Drastic enhancement by 438 cm^{-1} is noted for the in-plane ring deformation mode (ν_9) for the $TCyt^-$ radicals. The stretching frequency of C=O/S (ν_{28}) in Cyt/TCyt molecules is found to shifts downward by 101/79 cm^{-1} for Cyt^-/$TCyt^-$. The present calculation shows that the C-NH_2 stretching (ν_{24}) for the Cyt^- species is lowered by 193 with increases in IR intensity by a factor of ~ 7. The mode ν_{12} is found to decrease by 207 cm^{-1} and IR intensity increase by a factor of ~ 4 and the Raman band becomes polarized to depolarize in going from Cyt to Cyt^+. Due to the anionic radicalization of the Cyt and

TCyt molecules, the ν_{31} and ν_{33} modes are found to shift downward by 195/130 cm^{-1} and 178/152 cm^{-1} with increase in IR intensity and Raman activity in Cyt^{-}/$TCyt^{-}$. The frequency of the ω (NH_2) mode is increased drastically by 375 cm^{-1} in Cyt^{-} than that in Cyt. In case of the $TCyt^{-}$ species, the frequency of τ (NH_2) and ω (NH_2) modes are changed by 333 (lowering) and 753 (enhancement) cm^{-1} as compared to the TCyt molecule.

The complete vibrational assignments of wavenumbers have been made on the basis of PEDs. Reasonably good agreement of the calculated and observed vibrational spectra suggests the advantages of higher basis set for quantum chemical calculations. The MEP surfaces together with complete analysis of the vibrational spectra, both IR and Raman; help us to identify the structural properties of the studies species. The MEP surface suggests that the site close to the sulfur is the region of the most negative electrostatic potential. The electron density plot for molecule shows a uniform distribution.

Reference

1. Gräslund A, Ehrenberg A, Rupprecht A, Ström G, Crespi H (1975) Ionic base radicals in gamma-irradiated oriented non-deuterated and fully deuterated DNA. Int J Radiat Biol Relat Stud Phys Chem Med 28: 313-323.
2. Yan M, Becker D, Summerfield S, Renke P, Sevilla MD (1992) Relative abundance and reactivity of primary ion radicals in irradiated DNA at low temperatures. 2. single- vs double- stranded DNA. J Phys Chem 96: 1983-1989.
3. Wetmore SD, Eriksson LA, Boyd RJ, Eriksson LA (2000) Theoretical biochemistry: Processes and properties of biological systems, theoretical and computational chemistry, Elsevier, Amsterdam.
4. Barker DL, Marsh RE (1964) The crystal structure of cytosine. Acta Cryst 17: 1581-1587.
5. Furberg S, Jensen LH (1970) Crystal structure of thiocytosine. Acta Crystallogr B 26: 1260-1268.
6. Estrin DA, Paglieri L, Corongiu G (1994) A density functional study of tautomerism of uracil and cytosine. J Phys Chem 98: 5653-5660.
7. Susi H, Ard JS, Purcell JM (1973) Vibrational spectra of nucleic acid constituents-I: Planar vibrations of uracil. Spectrochim. Acta 20A: 725-733.
8. Nowak MJ, Lapinski L, Fulara J (1989) Matrix isolation studies of cytosine: The separation of the infrared spectra of cytosine tautomers. Spectrochim. Acta 45A: 229-242.
9. Yadav RA, Yadav PNS, Yadav JS (1988) Vibrational studies of biomolecules-II. 2-thiocytosine. Spectrochim. Acta 44A: 1201-1206.
10. Kwiatkowski JS, Leszczynski J (1996) Molecular structure and vibrational IR spectra of cytosine and its thio and selenoanalogs by density functional theory and conventional ab Initio calculations. J Phys Chem. 100: 941-953.
11. Subramanian V, Chitra K, Venkatesh K, Sanker S, Ramasami T (1997) Comparative study on the vibrational IR spectra of cytosine and thiocytosine by various semi-empirical quantum mechanical methods. Chem Phys Lett 264: 92-100.
12. Florian J, Baumruk V, Leszczynski J (1996) IR and Raman Spectra, tautomerism, and scaled quantum mechanical force fields of protonated cytosine. J Phys Chem. 100: 5578-5589.
13. Szczesniak M, Szczesniak K, Kwiatkowski JS, KuBulat K, Person WB (1988) Matrix isolation infrared studies of nucleic acid constituents. 5. Experimental matrix-isolation and theoretical ab initio SCF molecular orbital studies of the infrared spectra of cytosine monomers. J Am Chem Soc 110: 8319-8330.
14. Czerminski R, Kwiatkowski JS, Person WB, Szczepaniak K (1989) Quantum-mechanical studies of the structures of cytosine dimers and guanine-cytosine pairs. J Mol Struct 198: 297-305.
15. Jaworski A, Szczesniak M, Szczesniak K, KuBult K, Person WB (1990) Infrared spectra and tautomerism of 5-fluorocytosine, 5-bromocytosine and 5-iodocytosine. Matrix isolation and theoretical ab initio studies. J Mol Struct 223: 63-92.
16. Radchenko ED, Sheina GG, Smorygo NA, Blagoi Yu P (1984) Experimental and theoretical studies of molecular structure features of cytosine. J Mol Struct. 116: 387-396.
17. Stepanian SG, Sheina GG, Radchenko ED, Blagoi Yu P (1985) Theoretical and experimental studies of adenine, purine and pyrimidine isolated molecule structure. J Mol Struct 131: 333-346.
18. Gould R, Vincent MA, Hillier IA, Lapinski L, Nowak MJ (1992) A new theoretical prediction of the infrared spectra of cytosine tautomers. Spectrochim Acta 48A: 811-818.
19. Podolyan Y, Gorb L, Blue A, Leszczynski J (2001) A theoretical investigation of tautomeric equilibria and proton transfer in isolated and hydrated thiocytosine. J Mol Struct 549: 101-109.
20. Krishnakumar V, Balachandran V (2005) Analysis of vibrational spectra of 5-fluoro, 5-chloro and 5-bromo-cytosines based on density functional theory calculations. Spectrochim Acta A Mol Biomol Spectrosc 61: 1001-1006.
21. Rostkowska H, Nowak MJ, Lapinski L, Bretner M, Kulikowski T, et al. (1993) Theoretical and matrix-isolation experimental studies on 2-thiocytosine and 5-fluoro-2-thiocytosine. Biochim Biophys Acta 1172: 239-246.
22. Rostkowska H, Nowak MJ, Lapinski L, Bretner M, Kulikowski T, et al. (1993) Theoretical and matrix-isolation experimental studies on 2-thiocytosine and 5-fluoro-2-thiocytosine. Biochim Biophys Acta 1172: 239-246.
23. Singh R, Jaiswal S, Kumar M, Singh P, Srivastav G, et al. (2010) DFT study of molecular geometries and vibrational characteristics of uracil and its thio-derivatives and their radical cations. Spectrochim Acta A Mol Biomol Spectrosc 75: 267-276.
24. Singh R, Yadav RA (2014) Raman and IR studies and DFT calculations of the vibrational spectra of 2,4-Dithiouracil and its cation and anion. Spectrochim Acta A Mol Biomol Spectrosc 130: 188-197.
25. Yadav RA, Rani P, Kumar M, Singh R, Singh P, et al. (2011) Experimental IR and Raman spectra and quantum chemical studies of molecular structures, conformers and vibrational characteristics of l-ascorbic acid and its anion and cation, Spectrochim. Acta. 84A: 6-21.
26. Kumar M, Jaiswal S, Singh R, Srivastav G, Singh P, et al. (2010) Ab initio studies of molecular structures, conformers and vibrational spectra of heterocyclic organics: I. Nicotinamide and its N-oxide. Spectrochim Acta A Mol Biomol Spectrosc 75: 281-292.
27. Srivastava M, Rani P, Singh NP, Yadav RA (2014) Experimental and theoretical studies of vibrational spectrum and molecular structure and related properties of pyridoxine (vitamin B6). Spectrochim Acta A Mol Biomol Spectrosc 120: 274-286.
28. Srivastava M, Singh NP, Yadav RA (2014) Experimental Raman and IR spectral and theoretical studies of vibrational spectrum and molecular structure of Pantothenic acid (vitamin B5). Spectrochim Acta A Mol Biomol Spectrosc 129: 131-142.
29. Rani P, Yadav RA (2012) Ab initio determination of geometries and vibrational characteristics of building blocks of organic super-conductors: TTF and its derivatives. Spectrochim Acta A Mol Biomol Spectrosc 99: 303-315.
30. Poonam R, Gunjan R, Yadav RA (2015) Investigation of crystal structure, vibrational characteristics and molecular conductivity of 2, 3-dichloro-5, 6-dicyno-p-benzoquinone. Spectrochim. Acta 137A: 1334–1347.
31. Frisch MJ, Trucks GW, Schlegel HB, Scuseria GE, Robb MA (2010) Gaussian 09, Revision C.01, Gaussian, Inc., Wallingford CT.
32. Becke AD (1993) Density functional thermochemistry. III. The role of exact exchange. J Chem Phys 98: 5648-5652.
33. Lee C, Yang W, Parr RG (1988) Development of the Colle-Salvetti correlation-energy formula into a functional of the electron density. Phys Rev B Condens Matter 37: 785-789.
34. Frisch, Nielsen AB, Holder AJ, Gauss (2003) View user manual, Gaussian, Inc., Wallingford, USA.
35. Sundius T (2002) Scaling of ab initio force fields by MOLVIB. Vib. Spectrosc. 29: 89-95.
36. Keresztury G, Holly S, Varga J, Besenyei G, Wang AY, et al. (1993) Vibrational spectra of monothiocarbamates-II. IR and Raman spectra, vibrational assignment, conformational analysis and ab initio calculations of S-methyl-N, N-dimethylthiocarbamate. Spectrochim. Acta A 49: 2007-2017.

37. Durig JR, Little TS, Gounev TK, Gardnerjr JK, Sullivan JF (1996) Infrared and Raman Spectra, Conformational Stability, Vibrational Assignment, and Ab Initio Calculations of Chloro-methyl Isocyanate. J Mol. Struct 375: 83-94.

38. Amalanathan M, Rastogi VK, Joe IH, Palafox MA, Tomar R (2011) Density functional theory calculations and vibrational spectral analysis of 3,5-(dinitrobenzoic acid). Spectrochim Acta A Mol Biomol Spectrosc 78: 1437-1444.

39. Fukui K (1982) Role of frontier orbitals in chemical reactions. Science 218: 747-754.

40. Atkins PW (2001) Physical Chemistry, Oxford University Press, Oxford.

41. Mahadevan D, Periandy S, Karabacak M, Ramalingam S (2011) FT-IR and FT-Raman, UV spectroscopic investigation of 1-bromo-3-fluorobenzene using DFT (B3LYP, B3PW91 and MPW91PW91) calculations. Spectrochim Acta A Mol Biomol Spectrosc 82: 481-492.

42. Choi CH, Kertesz M (1997) Conformational Information from Vibrational Spectra of Styrene, trans-Stilbene, and cis-Stilbene. J Phys Chem A 101: 3823-3831.

43. Gunasekaran S, Arun Balaji R, Kumaresan S, Anand G (2008) Experimental and theoretical investigations of spectroscopic properties of N-acetyl-5-methoxytryptamine. Can J Anal Sci Spectrosc 53: 149-162.

44. Padmaja L, Ravi Kumar C, Sajan D, Joe IH, Jayakumar VS, et al. (2009) Density functional study on the structural conformations and intramolecular charge transfer from the vibrational spectra of the anticancer drug combretastatin-A2. J Raman Spectrosc 40: 419-428.

45. Kurtaran R, Odabasioglu S, Azizoglu A, Kara H, Atakol O (2007) Experimental and computational study on [2,6-bis(3,5-dimethyl-N-pyrazolyl)pyridine]-(dithiocyanato)mercury(II), Polyhedron, 26: 5069-5074.

46. Manolopoulos DE, May JC, Down SE (1991) Theoretical studies of the fullerenes: C34 to C70. Chem Phys Lett 181: 105-111.

47. Politzer P, Truhlar DG (1981) Chemical Applications of Atomic and Molecular Electrostatic Potentials, Plenum Press, New York.

48. Chattopadhyay B, Basu S, Chakraborty P, Choudhuri SK, Mukherjee AK, et al. (2009) Synthesis, spectroscopic characterization, X-ray powder structure analysis, DFT study and in vitro anticancer activity of N-(2-methoxyphenyl)-3-methoxysalicylaldimine. J Mol Struc 932: 90-96.

49. Singh UC, Kollman PA (1984) An approach to computing electrostatic charges for molecules. J Comput Chem 5: 129-145.

50. Connolly ML (1983) Solvent-accessible surfaces of proteins and nucleic acids. Science 221: 709-713.

51. Muthu S, Uma Maheswari J (2012) Quantum mechanical study and spectroscopic (FT-IR, FT-Raman, 13C, 1H, UV) study, first order hyperpolarizability, NBO analysis, HOMO and LUMO analysis of 4-[(4-aminobenzene) sulfonyl] aniline by ab initio HF and density functional method, Spectrochim. Acta 92A: 154-163.